12-2016

Development of Breast Tissue Phantoms for Enhanced Terahertz Imaging Utilizing Microdiamond and Nano-Onion Particles

Alec Walter
University of Arkansas, Fayetteville

Development of Breast Tissue Phantoms for Enhanced Terahertz Imaging Utilizing Microdiamond and Nano-Onion Particles

Development of Breast Tissue Phantoms for Enhanced Terahertz Imaging Utilizing Microdiamond and Nano-Onion Particles

Bachelor of Science in Electrical Engineering

Alec Bryant Walter

December 2016

University of Arkansas

Dr. Magda El-Shenawee
Thesis Advisor

Dr. Jingxian Wu
Department Honors Coordinator

Abstract

This thesis presents the work performed to develop tissue phantoms and a contrast agent that will be used in future research of terahertz time-domain imaging of breast tumor margins. Since an excised breast tumor can contain healthy fibrous and fatty tissues along with invasive ductal carcinoma (IDC), three phantom materials were developed. Solid phantom materials were made by using TX151 to solidify water in order to tune the refractive index and absorption coefficient of the fibrous tissue phantom and IDC phantom to the properties of freshly excised breast tissue. Various amounts of olive oil were added to the water prior to solidification to achieve these properties. As the fat tissue phantom required too much olive oil, a commercially available material was found that match the optical properties of fresh breast tissue. Both the refractive index and the absorption coefficient of the three phantoms were verified through the use of time-domain terahertz spectroscopy performed on the pulsed terahertz system at the University of Arkansas.

The proposed terahertz contrast agent was chosen from a group of carbon-based particles which included high pressure, high temperature synthetic diamond particles and onion-like carbon (OLC). To test the contrast agent, polyethylene tablets containing a known concentration of these particles were characterized using the time-domain terahertz spectroscopy. Two sizes of OLC (100-200nm) and five sizes of diamond particles (1-150um) were tested to determine the effects of varying particles sizes. Additionally, diamond particles with three types of treatments (pristine, irradiated and irradiated-annealed) were tested to determine what effects, if any, the treatments had. The particles effeteness as a contrast agent in lossy phantom tissue was tested by incorporating them into IDC phantoms. The results show that the 100nm OLC had potential as a terahertz contrast agent in breast cancer.

Table of Contents

I. Introduction

A. Motivation

In the United States, cancer is the second most prevalent cause of death [1]. To prevent and treat the large number of variations of cancer, numerous research is being performed. Breast cancer, specifically, is a common type of cancer that is researched due to its high incidence rates in women. It is estimated that one in eight women will develop some sort of breast cancer over their lifetimes [2].

The standard treatment option for breast cancer is typically a full mastectomy. This procedure removes the tumor along with the entirety of one or both breasts as well as the adjacent lymph nodes. However, if the breast tumor if found early enough that it is less than 5cm in diameter, the cancer can be removed with a breast conserving surgery, or lumpectomy [3]. If successfully performed, a lumpectomy will increase the survival rate of the patient to the same degree that a mastectomy would have while keeping the breast largely intact [4]. During a lumpectomy, the tumor is removed along with a small layer of the surrounding healthy tissue. This layer of healthy tissue, known as the tumor margin, is used after the surgery to determine if the surgery was successful.

The current gold standard of margin analysis is a pathological assessment by a histopathologist. This assessment involves embedding the tumor in a paraffin block before slicing and staining the tissue. From the thin slices of stained tissue, the pathologist characterizes the margin of the tumor as either positive, negative or close. A margin is considered positive when there is still cancerous tissue present at the surface of the margin, close when there is no cancerous tissue present at the surface of the margin but can be found within 0.5mm of the surface and negative when there is no cancerous tissue within 0.5mm of the surface of the margin. With conventional

lumpectomy procedures, 20-40% of excised tumors are found to have positive or close margins [3]. When a tumor is found to have a positive or close margin, a second surgery is typically required to remove any remaining cancerous tissue to prevent local recurrence of the cancer. While pathological assessment will result in a correct classification of the tumor margin, the entire process can take up to several days to complete. Thus, if it is determined that more tissue should be removed, the patient will have to undergo a second surgery. In order to mitigate this, intraoperative margin assessment techniques can be used while the patient is still under to roughly determine the classification of the tumor margins.

Previous work has shown that time-domain terahertz (THz) imaging is a promising new method of intraoperative margin assessment due to its ability to distinguish between cancerous tissue and healthy fibrous and fatty tissues [6], [7]. Since obtaining fresh tissue to work with can be difficult outside of a hospital, tissue phantoms are required. Tissue phantoms, or tissue analogs, are materials that, for a specific type of imaging, can mimic a specific type of tissue. Phantoms can be used to make models to test new imaging techniques and methods before they are used on actual tissue. As THz technologies are still relatively new, little work has been performed on the development of broadband THz tissue phantoms. Since a breast tumor will commonly be composed of healthy fibrous and fatty tissues along with cancerous tissue, this work focused on developing phantoms for all three tissues types.

THz imaging, unlike many other imaging techniques, can distinguish between fibrous and cancerous tissues due to the different tissue types having different THz optical properties [8]. However, the difference between these properties are relatively small and could lead to incorrect margin characterization when using THz imaging. One method that could reduce this risk would be to utilize a contrast agent. If a contrast agent was to be localized to the cancerous tissue prior

to imaging, the relative difference in optical properties between the cancerous tissue and the healthy could be increased. This would allow for more accurate margin characterization using THz imaging. Since, like with the phantoms, little work had been done on identifying THz contrast agents, this work will also focus on identifying a potential contrast agent.

B. Pulsed Terahertz Spectroscopy and Imaging System

This research was performed using a TPS Spectra 3000, a commercially available pulsed THz spectroscopy and imaging system available from TeraVIEW, Ltd. [9]. The system is capable of operating in either a reflection or transmission mode by use of different system module. A basic diagram of the system's signal path while setup for transmission measurements is found in figure 1.1.

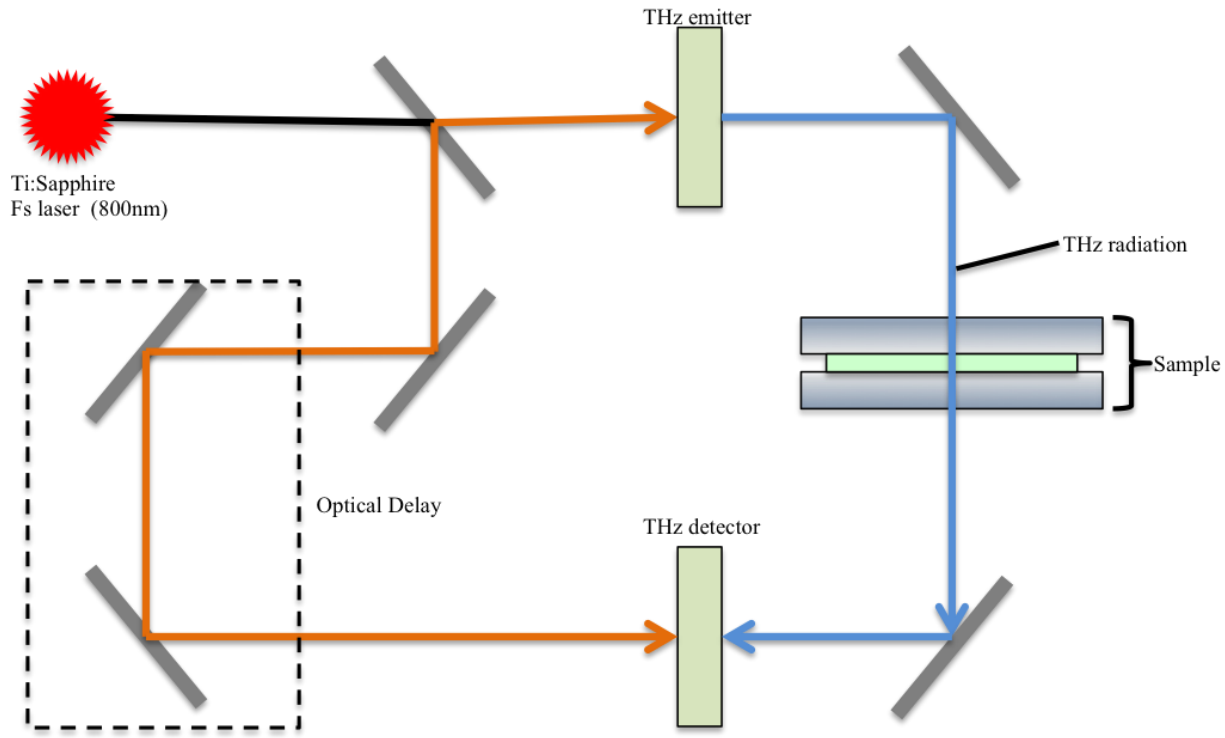

Figure 1.1. Diagram of the TPS Spectra 3000 in transmission mode.

The system produces the time-domain THz signal by first exciting a DC-biased GaAs antenna with an 800nm Ti:Sapphire laser pulse. Due to this excitation, the antenna produces a time-

domain THz pulse with a width that is roughly 500fs. The path of the signal is controlled through a series of optical mirrors such that it passes through the sample under test and onto the THz receiver. Like the source, the receiver is a GaAs antenna which is excited from a portion of the original laser pulse that had been split off and passed through an optical delay. When the THz signal is incident on the receiver, a voltage is generated across the antenna which is recorded as the measured signal. By performing Fourier transform on this measured time-domain pulse, a spectrum of complex frequency-domain values can be obtained from roughly 100GHz to 4THz.

II. Development of Breast Tissue Phantoms

While terahertz (THz) imaging has shown potential to act as an intraoperative technique to classify breast tumor margins, it can be difficult to acquire fresh human tissue to work with [6], [7]. To mitigate the need for fresh tissue, phantom materials which mimic the desired properties of the tissues can be used instead. While there has been a lot of work in developing tissue phantoms at the lower microwave frequencies, little work has been performed on THz phantoms [10]-[12].

In one such previous work, Walker tested various concentrations of TX151 and naphthol green to determine if either material could work as a THz tissue phantom [13]. TX151 was added to water such that the volume ratios were 1:4, 1:2 and 1:1 while the naphthol green dye was added to water such that either 10, 15 or 20 wt.% of the sample was the dye. Using various thicknesses of each sample, the refractive indices and absorption coefficients were measured and compared to the properties of fatty tissue, skin and striated muscle. From these results, it was found that the material with a 1:2 ratio of TX151 had an absorption coefficient consistent with muscle while the material with a 1:1 ratio had an absorption coefficient consistent with skin and a refractive index that matched adipose tissue. While the sample whose mass was either 15 and 20% naphthol green dye had absorption coefficients similar to adipose tissue, none of the naphthol green samples has a refractive index similar to compared tissues.

A second work by Reid tested the viability of using an emulsion as a THz tissue phantom [14]. Different emulsions were made by varying the amount of safflower oil added to the water from 0 wt.% to 100 wt.%. After characterizing each emulsion, it was found that the as the concentration of safflower oil increased, both the refractive index and absorption coefficient decreased. While the resulting properties were not directly compared to the properties of any fresh tissue, the range

observed for both the refractive index and absorption coefficient covers the properties commonly found for fresh tissue.

A. TX151-Based Phantoms

The first attempt at making THz phantoms for breast tissues utilized the same procedures described by Walker [13] for his TX151 phantoms. TX151 was chosen as it was the only material that had been shown to produce viable, solid phantoms; a characteristic that would be required to produce three-dimensional tumor margin models.

Following the procedure, three potential phantoms were made using volume ratios of TX151 to water of 1:1, 1:1.5 and 1:2. This was done by utilizing a magnetic mixer and a stir bar to mix the TX151 into the water. Unfortunately, the rate of solidification caused by the TX151 is dependent on the amount of TX151 use and the temperature of the water, with colder water slowing the solidification. For all four of the materials that were made, the rate of solidification was so rapid that most the powder couldn't even be mixed in.

In order to get materials that utilized the entire desired amount of TX151, the temperature of the water used was lowered to right above the freezing point. Using the cold water, most the powder was able to mix in to each of the potential phantoms. Unfortunately, while this method did slow down the solidification process enough to allow the magnetic mixer to mix in most of the TX151, not all of it could interact with water before it solidified. This caused small pockets of powder to permeate throughout each of the potential phantom materials.

Despite the powder not being completely incorporated into the materials, there was no other method, despite lowering the amount of TX151 used, that could slow down the solidification process further. Thus, to get an idea of the THz properties of these materials, each of them were characterized using THz transmission spectroscopy. As the results of the spectroscopy are

dependent on the thickness of the sample used, a liquid sample holder has utilized to guarantee the thickness of the sample. As can be seen in figure 2.1, the liquid sample holder consists of two quartz window and a plastic spacer with a known thickness. The sample is placed between the two windows which are separated by the spacer. The windows are then compressed such that the space between them is fixed to be the thickness of the spacer. For these measurements, the width of the spacer used was 500um. Quartz is used for the windows as it is highly transparent in the terahertz range and thus won't cause a noticeable attenuation of the terahertz signal.

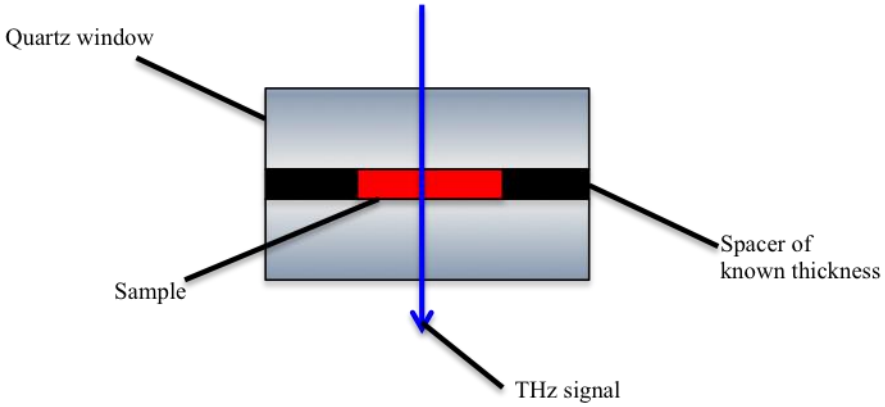

Figure 2.1. Model representation of the liquid sample holder used for THz spectroscopy.

The actual process of time-domain terahertz spectroscopy consists of first taking a reference measurement and then the sample measurement. Since the sample measurement includes the effects of the two quartz windows when using the liquid sample holder, the reference measurement is taken through both windows without a spacer between them. After the measurements are taken, the time domain results are processed with a Fast Fourier Transform to acquire the reference and sample frequency dependent electric fields. Then, by dividing the sample electric field by the reference electric field, the effect that the sample itself had on the measured electric field can be found.

Then, to obtain the refractive index and absorption coefficient of the sample, error analysis is performed at each frequency point for both the magnitude and phase. The error analysis involves

taking the measured magnitude and phase of the electric field and subtracting from it a theoretical value. The theoretical values used are dependent on the unknown optical properties of the sample. Thus, combinations of optical properties from a range of potential refractive indices and absorption coefficients are used to produce different theoretical values. These theoretical values are used in the error analysis and the resulting errors are analyzed to find the correct combination of refractive index and absorption coefficient. The correct refractive index and absorption coefficient for a given frequency point are thus the ones whose theoretical electric field value is the closest to the measured field.

Using this method, the optical properties for each of the TX151-and-water materials were determined. To determine if this method could produce a material that could serve as a phantom for either IDC, fibrous breast tissue or fatty breast tissue, the properties of each of the materials were compared to the known optical properties of fresh breast tissue [8]. As can be seen from figure 2.2, the refractive indices of the three compositions were relatively well matched to that of the fresh IDC tissue while their absorption coefficients were much higher than any of the fresh tissues. Also, the optical properties of the three materials showed little variation between one another. This is most likely due to the rapid solidification only allowing a similar amount of TX151 to be incorporated while the rest was trapped in the material still in powder form. This inhomogeneity in the materials is also the most likely cause of the strange spike in both the refractive index and absorption coefficient exhibited around 1THz in the 1:1 composition. Due to the issue caused by the rapid solidification and the resulting TX151 powder deposits, it was determined that materials made solely from TX151 and water were unable to produce usable terahertz imaging, breast tissue phantoms.

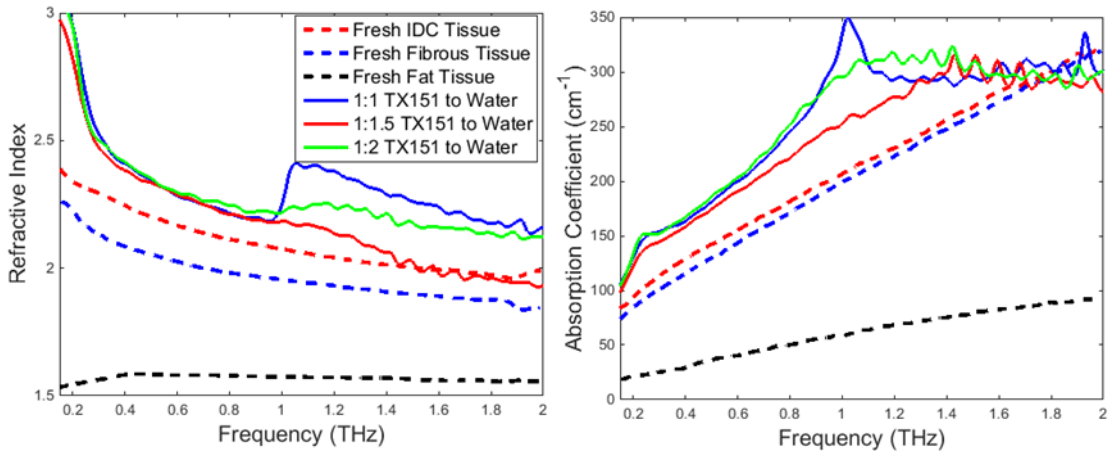

Figure 2.2. The refractive index and absorption coefficient of materials made from TX151 and water compared to freshly excised breast tissue [8].

B. Emulsion-Based Phantoms Predictions

With the TX151-based materials proving to be unsuitable to act as phantoms for any of three main types of breast tissue, focus was instead shifted to the safflower emulsions presented by Reid [14]. By altering the ratio of water and oil used to make the emulsion, the THz optical properties of these liquid phantoms can be altered over a wide range. Unfortunately, by being liquid in nature, these emulsion phantoms are incapable of being used to produce an imaging model for a breast tumor margin. But, even though liquid emulsions are not directly useable, the wide range of properties they offer is still desirable. Thus, in order to produce a solid phantom with the desired properties, the feasibility of a TX151 solidified emulsion was investigated.

As safflower oil can be expensive, especially in large quantities, olive oil was used as a replacement. To make sure that replacing safflower oil with olive oil wouldn't alter the range of properties that the emulsion could have, olive oil was characterized using THz spectroscopy. As can be seen in figure 2.3, olive oil has a very similar refractive index and absorption coefficient to the published optical properties of safflower oil [ref needed].

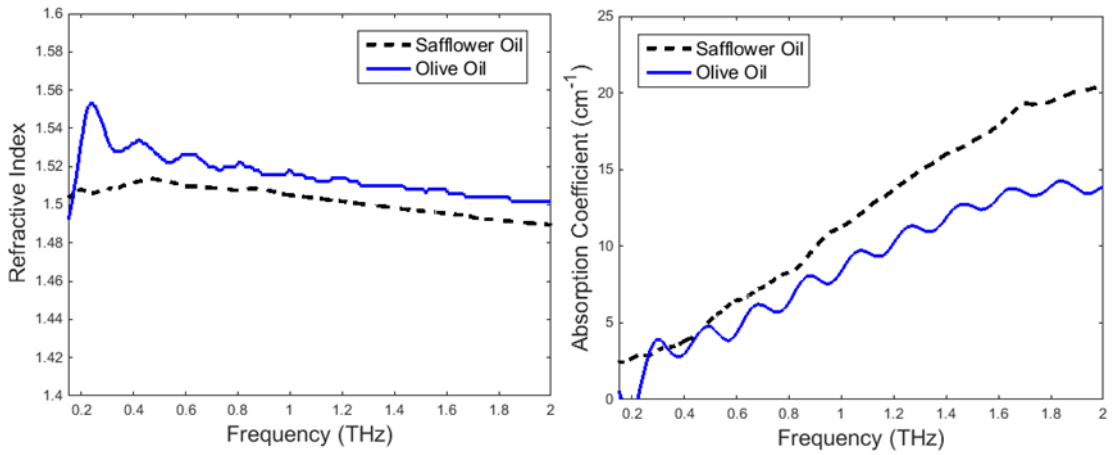

Figure 2.3. The refractive index and absorption coefficient of olive oil and safflower oil [14].

When making an emulsion, a surfactant is needed to allow the oil and water to mix together. They do this by lowering the surface tension which normally prevents oil and water from forming a stable mixture. While the safflower emulsion phantoms utilized powdered surfactants like SDS, this work instead utilized a neutral, liquid detergent. Besides being more readily available, using a neutral detergent as the surfactant in emulsion phantoms has precedence in microwave frequency breast tissue phantoms [10].

With the optical properties of olive oil being so similar to those of safflower oil, emulsions using olive oil can be expected to have similar properties as those using safflower oil. Using this similarity, the necessary amount oil for each phantom type could be roughly predicted. However, the effects that the addition of TX151 would have on the properties of the resulting material are unknown. To reduce the number of possible TX151 and olive oil ratios that would need to be tested, a method to predict the necessary ratios of components required to achieve specific optical properties was uses.

It has been shown that the permittivity of a heterogeneous compound can be related to the permittivities of the dispersing and dispersed mediums. While there are numerous equations that relate the permittivities of the component materials and the resulting material, they are specific to

the shape of the dispersed medium. For the emulsion phantoms, the oil can be taken to be the dispersed medium leaving the combination of everything else to be the dispersing medium. Since olive oil, after being dispersed in water with a surfactant, will form micelles that are roughly spherical in nature, Bottcher's equation for spherical particles was used [15].

$$v_2 = \frac{(\tilde{\epsilon}-\tilde{\epsilon}_1)(2\tilde{\epsilon}+\tilde{\epsilon}_2)}{3\tilde{\epsilon}(\tilde{\epsilon}_2-\tilde{\epsilon}_1)} \tag{2-1}$$

This equation relates the complex permittivity of the heterogeneous material $\tilde{\epsilon}$, the complex permittivity of the dispersing medium $\tilde{\epsilon}_1$, and the complex permittivity of the dispersed medium $\tilde{\epsilon}_2$ to the volume packing fraction of the dispersed medium v_2. This volume packing fraction represents the volume of the dispersed medium per unit cell of the heterogenous mixture. While the true value of volume packing fraction can be difficult to obtain, if the dispersed medium is assumed to be evenly distributed throughout the heterogeneous material, the volume packing fraction can be taken to be the percent volume of the dispersed medium in the heterogeneous mixture.

In order to solve Bottcher's equation for the heterogeneous permittivity, the equation can be rearranged into a quadratic form.

$$0 = 2\epsilon^2 + (3v_2(\epsilon_1 - \epsilon_2) + \epsilon_2 - 2\epsilon_1)\epsilon - \epsilon_1\epsilon_2 \tag{1-2}$$

To solve this equation for the electrical properties of a heterogeneous mixture with a given volume percentage of oil, the electrical properties of both the olive oil and the water-surfactant-TX151 dispersing are required. While the THz properties of the olive oil are known due to previous spectroscopy, the properties of the dispersing medium are dependent on the ratio of water, TX151 and surfactant.

Though the properties of this base material could be easily measured with THz spectroscopy, the composition of the dispersing material had to first be decided on. The main influencing factor of

this composition is the rate of solidification due to the ratio of TX151 to water. Too much TX151 with respect to water and clump of powder will form, too little and the mixture won't completely solidify. In order to determine an appropriate amount of TX151, 50mL of deionized water and 3mL of neutral detergent were combined with five different amounts of TX151: 5.55, 7.54, 12.5, 16.67 and 21.43 grams corresponding to 10, 15, 20, 25, and 30 wt.% respectively. Each composition was made using a magnetic mixer to achieve as even a distribution as possible. After making the different materials, it was found that the 10 and 15 wt.% additions of TX151 did not allow the material to completely solidify and instead formed soft, gelatinous-like materials that were incapable of supporting their own weight and thus were inappropriate to use as phantoms. While the other three compositions produced usable solids, it was unknown if any of them solidified too fast and thus contained pockets of undistributed powder. To determine this, each material was sliced open and viewed with a microscope under low levels of magnification. As can be seen in figure 2.4, the material with a 30 wt.% addition of TX151 contained large clumps of powder that hadn't reacted with water. The 25 wt.% addition, while better than the 30 wt.%, also contained clumps of undistributed powder. As the 20 wt.% addition of TX151 produced no noticeable clumps of powder and resulted in a completely solid material, it was chosen for the composition of the dispersing material.

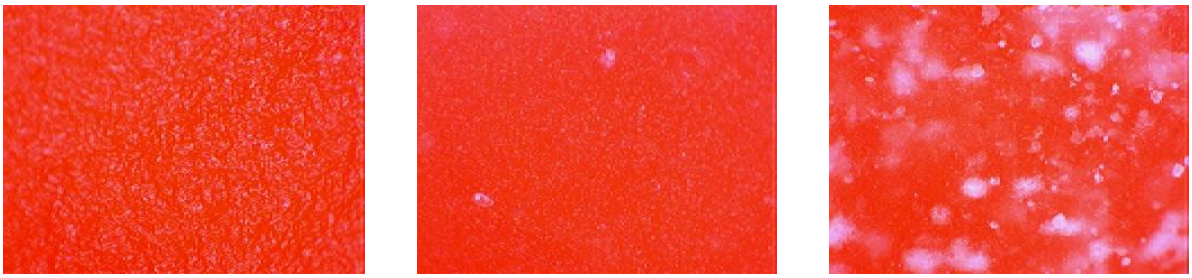

20 wt.% TX151 25 wt.% TX151 30 wt.% TX151

Figure 2.4. Microscope images of potential base materials with either a 20, 25 or 20 wt.% addition of TX151.

In order to obtain the electrical properties of the chosen material, the material was characterized using time-domain THz spectroscopy. With the properties of both the dispersing and dispersed mediums known, Bottcher's equation was utilized to predict the properties of potential heterogenous mixtures. The effects of different amounts of olive oil were predicted by altering the volume packing fraction which corresponds to altering the percent volume of olive oil in the heterogenous material. The resulting properties were then compared to the published THz properties of fresh breast tissue to determine the approximate amount of olive oil to include to achieve the desired properties [8].

C. Invasive Ductal Carcinoma Phantom Development

Using the predicted optical properties from Bottcher's equation, it was determined that to achieve optical properties similar to those of fresh invasive ductal carcinoma (IDC) the percent volume of olive oil used needed to be between 10 and 20% [15]. To validate this prediction, three different emulsion phantoms were made with 50mL of water, 3ml of neutral detergent, 12.5g of TX151 and either 6.0, 9.4 or 13.2mL of olive oil corresponding to 10, 15 and 20 vol.% of olive oil respectively. After characterizing each of the phantoms, their frequency-dependent refractive index and absorption coefficient were plotted with and compared to the published properties of fresh IDC, as seen in figure 2.5 [8].

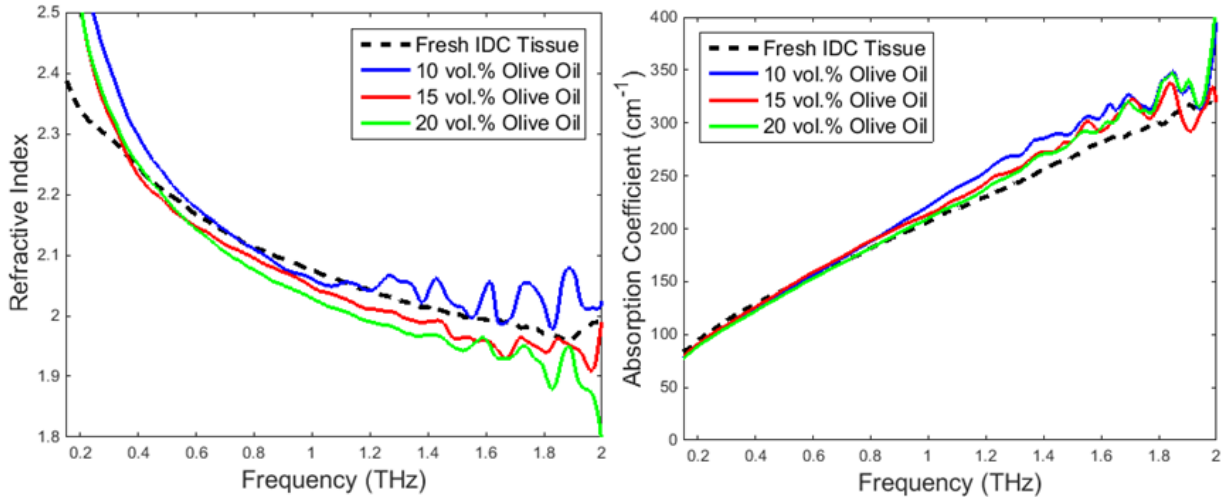

Figure 2.5. The refractive index and absorption coefficient of the initial IDC phantoms compared to freshly excised IDC tissue [8], [16].

While the resultant properties of all three phantoms showed strong agreement with the predictions by having similar properties to fresh IDC, there are some discrepancies between the two. For all three phantoms, the refractive indices tended to be lower than that of fresh tissue except for at frequencies lower than 0.4THz due to a low frequency spike discussed in section 2.F. The absorption coefficients, on the other hand, tended to be higher than that of fresh IDC with the differences becoming more pronounced at higher frequencies. While these phantoms provided a good starting point, the properties of the phantom need to be more finely tuned to the properties of the tissue. Since simply altering the amount of olive oil used to make the phantom will shift both the refractive index and absorption coefficient in the same direction, the difference between the phantom and tissue properties could not be fixed by simply changing the amount of oil in the phantom.

In order to find a phantom composition that better mimicked the optical properties of fresh IDC, salt (NaCl) was added to the phantom as it is a common component used in microwave phantoms to alter the conductivity [11]. As the absorption coefficient is related to the conductivity of the material, it was believed that the salt could be used to tune the absorption coefficient to the

required value after matching the refractive index. As the phantom with the 10 vol.% addition of olive oil had the best matched refractive index out of the three previously tested phantoms, its composition was used to test the effects of adding salt. Three new phantoms were made with an addition of either 2, 4 or 6g of salt. After making the new phantoms, they were characterized and their properties were compared to fresh IDC.

From the results, it was found that both the refractive index and absorption coefficient tended to increase as the amount of salt included in the phantom increased. However, the increase in absorption caused the signal to attenuate down to the level of noise. To keep the absorption of the material low enough and to determine if the increase provided by the salt could be used to obtain a material that better mimics fresh IDC, salt was added to the emulsion composition developed for the fibrous breast tissue phantom. This was done because the fibrous tissue phantom has optical properties lower than that of IDC (see section 2.D). Three new materials were made using the composition for the fibrous tissue phantom and either a 2, 4 or 6g addition of salt. As can be seen by figure 2.6, the increase in optical properties provided by even the largest addition of salt was too small to reach the properties of fresh IDC.

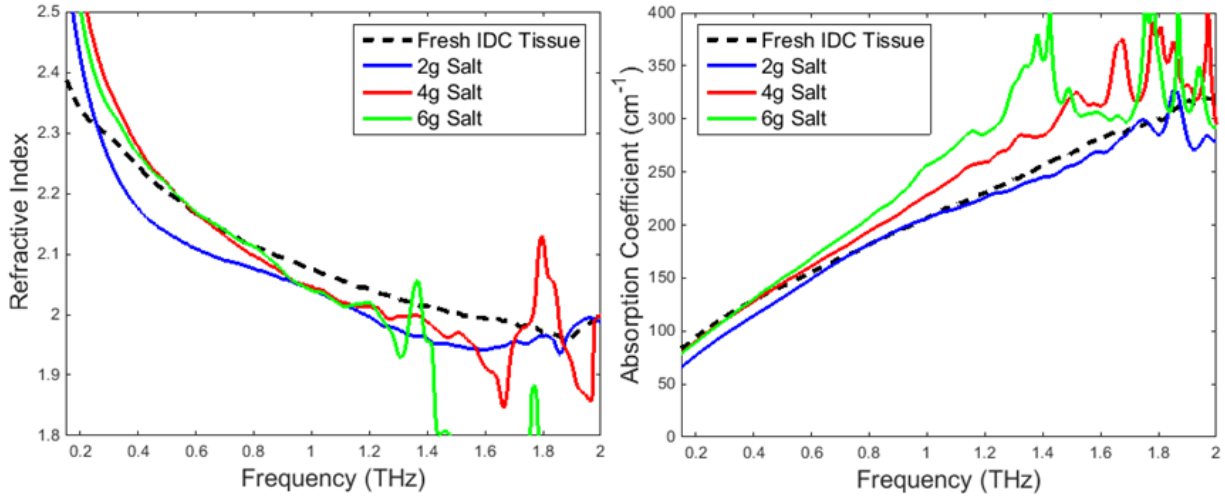

Figure 2.6. The refractive index and absorption coefficient of fibrous tissue phantoms with additions of salt compared to freshly excised IDC tissue [8].

While, theoretically, further increasing the amount of salt added could result in the desired properties, unfortunately high levels of salt tend to destabilize emulsions resulting in a quickening of the dissociation of the water and oil and thus decreasing the usable lifetime of the phantoms. Since increasing the amount of salt wasn't an option, the amount of oil used was instead decreased. Two different amounts of oil, 10 and 13.2 mL, were utilized along with the previous amounts of salt. Without salt, the 13.2mL compositions had a refractive index that tended to be lower than that of fresh IDC while having an absorption coefficient that closely matched. The 10mL composition without salt, on the other hand, tended to have a refractive index that matched fresh IDC and an absorption coefficient that was too large. Unfortunately, these compositions tended to have very noisy and inconsistent optical properties. For all of the previous cases, the salt was added into the TX151 powder and thus added in the mixture during the solidification phase. If the solidification happened too rapidly to allow the salt to completely dissolve into the material, salt crystals would be studded throughput the material and cause the inconsistent properties.

To resolve this issue, three steps were taken. The first was that the salt was grinded down using a mortar and pestle to reduce the grain size and thus increase the rate that the salt dissolved in water. The second step was that the, now finer gain, salt was added into the emulsion before the TX151 and allowed to dissolve completely. Lastly, the amount of salt added into the emulsion phantom was decreased. This was done not only to reduce the inconsistencies in the optical properties but also to decrease any of the negative effects the salt has on the phantom lifetime. Using these three methods, emulsion phantoms with either 13.2 or 10mL of olive oil and either 1, 2 or 3g of salt were made. After characterizing the potential phantoms and comparing their optical properties to that of fresh invasive ductal carcinoma (figure 2.7), it was found that while

the noise had been greatly reduced, none of the compositions were able to mimic both the refractive index and absorption coefficient of IDC and could at most only match one.

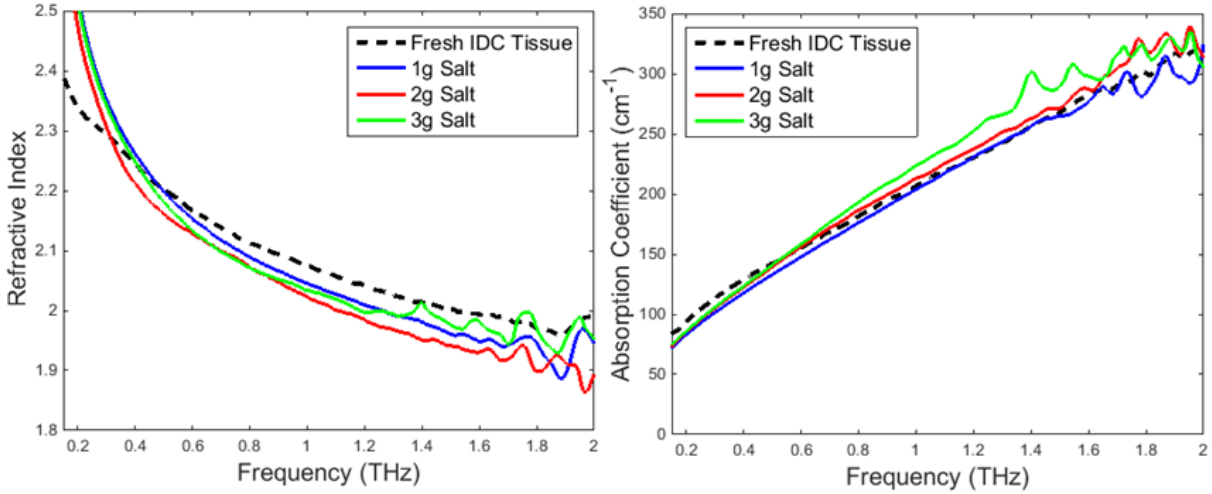

Figure 2.7. The refractive index and absorption coefficient of IDC phantoms with 10mL of olive oil and additions of salt compared to freshly excised IDC tissue [8].

As including salt in the emulsion composition was both unable to achieve the desired properties and resulted in lower usable lifetimes for the materials, the use of salt was halted. Instead the ratio between the amount of olive oil and surfactant used in the materials was altered to change the optical properties of the materials to achieve the desired optical properties. Using the previous composition with 10 vol.% of oil as a base, three new potential phantoms were made. From the original 3mL of surfactant, the amount of surfactant in each phantom was increased to either 4, 5 or 6mL. This range of increase corresponded to changing the ratio of oil to surfactant from 2:1 to 1:1. After characterizing these materials their optical properties were compared to those of fresh IDC [8]. By decreasing the ratio of olive to detergent both the refractive index and absorption coefficient were lowered with the decrease in the refractive index being larger than that the decrease in the absorption coefficient.

Since the decrease provided by the decreased oil to surfactant ratio lowered the refractive index of the tested materials to below that of fresh IDC, the amount of olive oil utilized was lowered.

To prevent the decreased amount of olive oil from increasing the absorption coefficient by too much and thus overshooting the desired values, the composition with an oil to surfactant ratio of 1 to 1 was used as it had the lowest absorption coefficient and thus could take a larger increase than the other materials. Using the 1:1 ratio, three new potential phantoms were made using 5, 4 or 3mL of olive oil and surfactant. The three materials were then characterized using transmission THz time-domain spectroscopy to obtain their optical properties. As seen in figure 2.8, the effect of decreasing the amount of oil yielded the expected results as both the refractive index and absorption coefficient increased. This increase resulted in the material with 5mL of olive oil and detergent having optical properties that closely resembled those of fresh IDC.

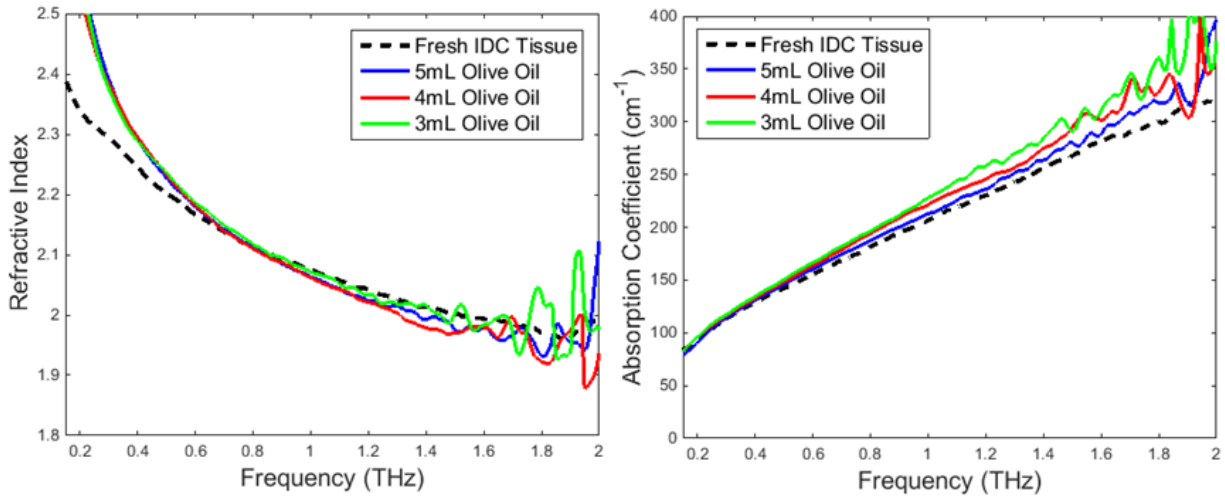

Figure 2.8. The refractive index and absorption coefficient of IDC phantoms with a 1:1 ratio of oil and detergent compared to freshly excised IDC tissue [8], [16].

To gain a better understanding of both the refractive index and absorption coefficient of the 5mL phantom, nine new phantoms were made using the same composition. After characterizing all of the new phantoms, their optical properties were averaged together and the standard deviation was obtained. From these values, a 95% confidence interval was obtained for both the refractive index and absorption coefficient to roughly predict the range of properties that any given phantom made with this composition could have. As seen in figure 2.9, the absorption coefficient

of the 5mL phantom closely matches that of fresh IDC over the entire frequency range of 0.15 to 2 THz. Like the absorption coefficient, the refractive index of the 5mL phantom is well matched to that of the fresh tissue. The main discrepancy between the two is the low frequency spike in refractive index of the phantom discussed in section 2.F. For both the refractive index and absorption coefficient, there is a noticeable increase in the variance between different phantom samples near 2 THz. This is most likely due to the high absorption of the material at this frequency attenuating the signal and causing it to approach the noise level and not from any intrinsic property of the phantom. Due to how well the 5mL phantom matched the properties of fresh IDC, it was chosen to be the IDC phantom.

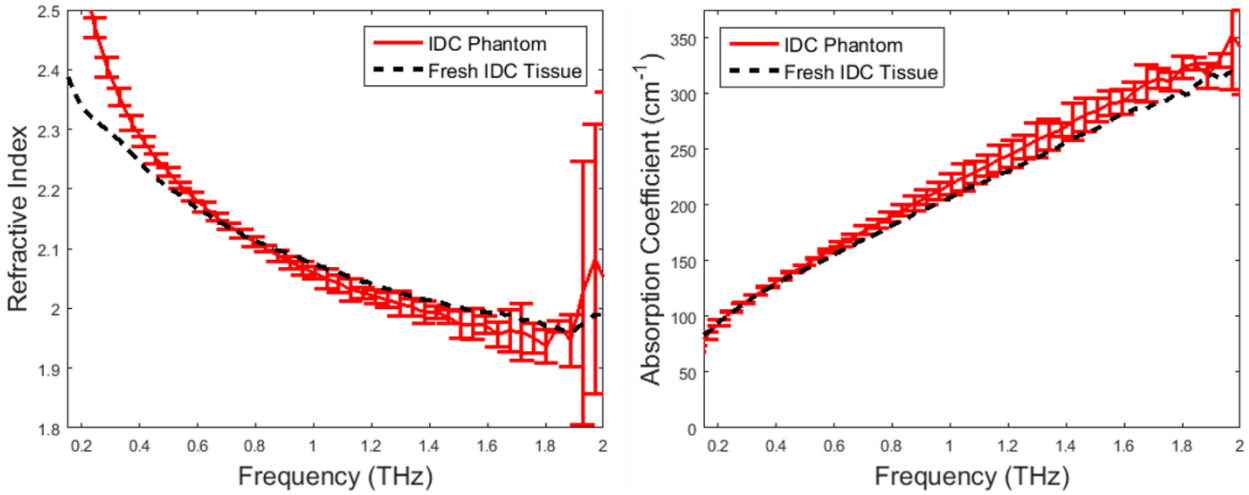

Figure 2.9. 95% confidence intervals for the refractive index and absorption coefficient of the final IDC phantom compared to freshly excised IDC tissue [8], [16].

D. Fibrous Tissue Phantom Development

Using the predicted optical properties from Bottcher's equation, it was found that an emulsion material with a percent volume of olive oil between 25 and 40% would yield optical properties close to those of fresh fibrous breast tissue [15]. To verify this prediction, four different compositions were made using the base material used in the predictions and an inclusion of either 17.6, 22.8. 28.6 or 34.5mL of olive oil which corresponds to a 25, 30, 35 or 40 vol.%

addition, respectively. The first round of potential phantoms made in this way were unable to be characterized as the oil did not completely disperse throughout the material. This was due to a lack of surfactant with respect to the amount of oil used. To rectify this, the amount of detergent used was increased from 3mL to 8.8mL. This was done with the understanding that the increase in surfactant could cause a discrepancy between the predicted and measured optical properties. With this new composition, the four phantoms were successfully made as the increased amount of surfactant appeared to allow for a complete dispersion of the olive oil. Each of the four phantoms were then characterized suing the THz transmission, time-domain spectroscopy procedure outlined previously in this chapter. As seen in figure 2.10, it was found that while the increased level of surfactant resulted in lower optical properties than what was predicted, there was still relatively good match between the four materials and fresh fibrous breast tissue for both the refractive index and absorption coefficient. In particular, the emulsion composition with 17.6mL of olive oil had optical properties closest to that of fresh fibrous tissue.

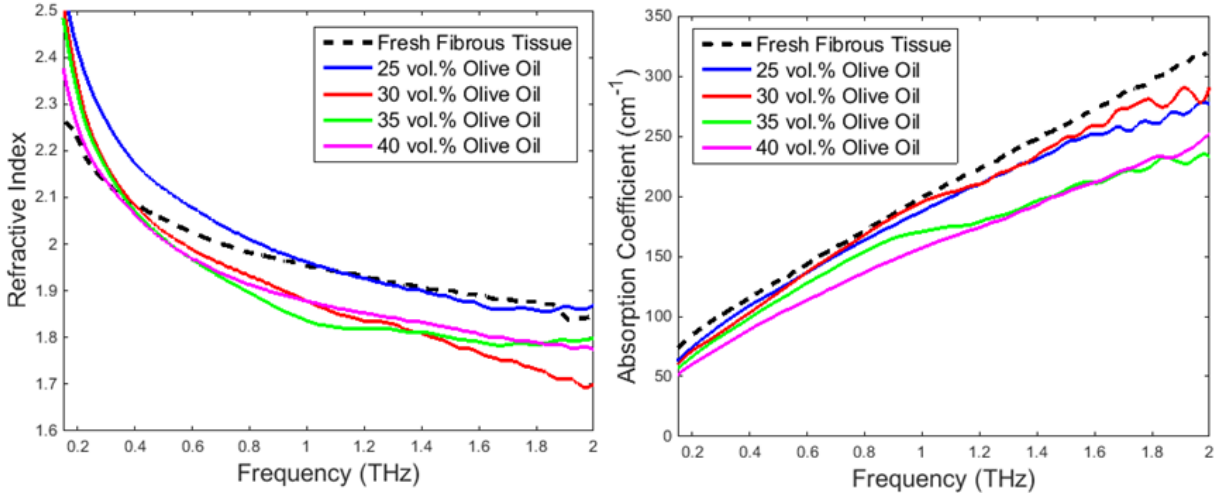

Figure 2.10. The refractive index and absorption coefficient of the initial fibrous tissue phantoms compared to freshly excised fibrous breast tissue [8], [16].

To gain a better understanding of the optical properties of the phantom with 25 vol.% of oil, nine more phantoms with the same composition were made and characterized. The optical properties

of the ten phantoms were averaged together to obtain the average refractive index and absorption coefficient and their respective standard deviations. From those, a 95% confidence interval for each property was obtained to gauge the range of properties that any given phantom made with this composition could have.

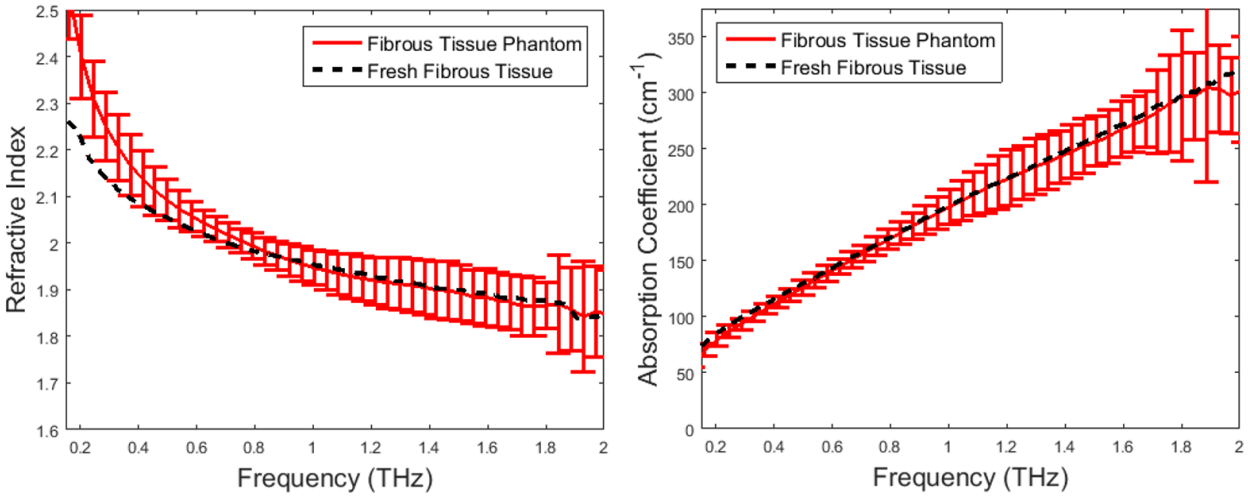

Figure 2.11. 95% confidence intervals for the refractive index and absorption coefficient of the final fibrous tissue phantom compared to freshly excised fibrous breast tissue [8], [16].

As seen in figure 2.11, the 95% confidence intervals for the 25 vol.% oil composition match the desired properties of the fresh fibrous breast tissue. The similarities between the refractive indices and absorption coefficients are strong enough that they appear to be nearly identical. Unfortunately, the phantom does exhibits the low frequency spike in refractive index, discussed in section 2.F, which causes the refractive index of the phantom to deviate away from that of the fresh tissue. Additionally, while the average optical properties of the phantom match well at higher frequencies, the variance between different phantom with this composition increases near 2 THz. The increased variance is most likely due to the high absorption of the material attenuating the signal to the point where it has begun to reach the noise level. Despite the minor inconsistencies, how well the 25 vol.% phantom mimicked the properties of fresh fibrous breast tissue lead to it being chosen as the fibrous tissue phantom.

E. Fat Tissue Phantom Development

To find the approximate amount of oil to include in an emulsion phantom for fatty breast tissue, the results of Bottcher's equation were once gain used [15]. However, due to fresh fatty breast tissue having both a relatively low refractive index and absorption coefficient, the amount of oil required would need to be between 80 and 90%. Since the amount of oil in the emulsion would be greater than the amount of water, the oil would no longer be dispersed in the water (an oil-in-water emulsion) and instead the water would be dispersed in the oil (a water-in-oil emulsion). While this difference in the makeup of the emulsion is not inherently troublesome, it poses a major issue when TX151 is used to solidify the emulsion. This is because TX151 reacts with water to solidify and does not solidify when mixed with olive oil. In the oil-in-water emulsions, the TX151 and water solidify around the oil and trap in in the resulting solid. In the water-in-oil emulsion, however, the dispersed water would solidify with the TX151 and a majority of the oil would not be trapped in the solid. This loss of oil would prevent the resulting material from achieving the low properties of the fresh fatty tissue.

As a solid emulsion phantom could not be made using the same method used to develop the IDC and fibrous tissue phantoms, some other method had to be found. However, instead of searching for a new mechanism of solidification that would work on the olive oil, commercially available solid emulsions were explored. The first material that was tested was animal lard as lard is predominantly composed of rendered animal fat and was thus theorized to have optical properties similar to human fat tissue. After characterizing a sample of animal lard, both its refractive index and absorption coefficient (figure 2.12) were found to be lower than those of fresh fat tissue. While the refractive index of the lard was still relatively close to that of the fresh tissue, the absorption coefficient was especially lower than the tissue. This difference in

absorption coefficients is most likely due to the lard containing little to no water when compared to fresh tissue as water tends to be highly assortative in the THz band [14].

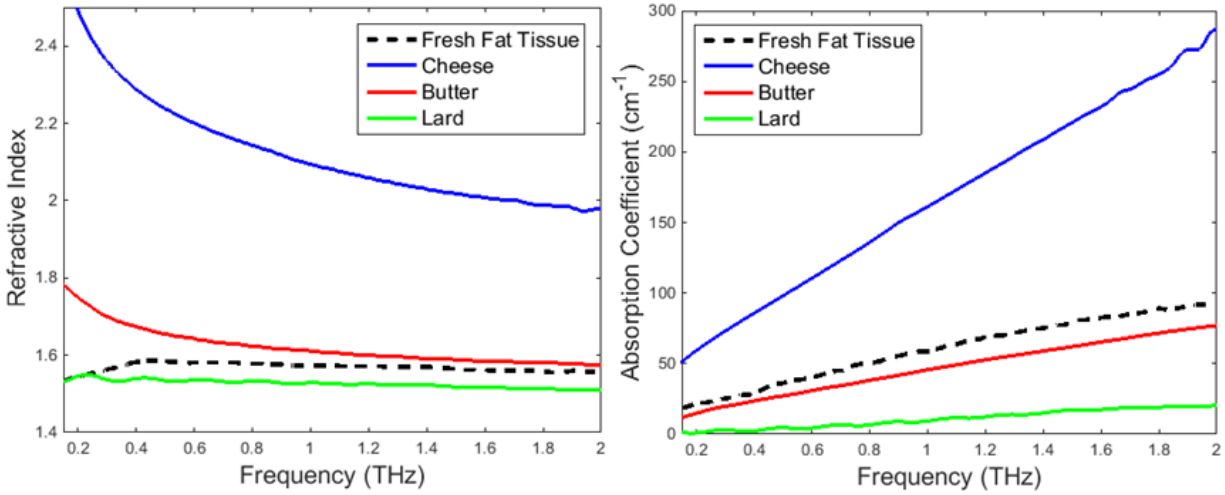

Figure 2.12. The refractive index and absorption coefficient of the three materials tested to be fat tissue phantoms compared to freshly excised fatty breast tissue [8].

The second material that was tested was a processed cheese product. Cheese was chosen due to it being mainly made of water, milk fat and whey protein and thus having a composition that closely resembled that of human tissue as tissue is predominantly made up of water, lipids and protein [17], [18]. Due to this resemblance in composition, it was predicted that the cheese would have optical properties that resembled fresh fat tissue. After the spectroscopy, however, it was found that both the refractive index and absorption coefficient of the processed cheese were much greater than those of fresh fat tissue (figure 2.12). This large discrepancy is most likely due to the cheese containing much more water, relative to amount of oil, than fatty breast tissue.

The last material that was tested was unsalted butter. Butter was primarily chosen to be tested as it is an emulsion of water dispersed throughout milk-fat. As average butter is roughly 81% oil, a composition that falls within the original predicted range for the required amount of olive oil, it was predicted that butter would have properties that were close to or within the range predicted for TX151 phantoms with a similar amount oil. After obtaining the optical properties of the

butter through THz time-domain spectroscopy, the results were compared to the properties of fresh fatty tissue. As seen in figure 2.12, butter was found to have a refractive index that is only slightly higher and an absorption coefficient slightly lower than that of fresh tissue. Due to how closely the optical properties of the butter resembled those of the fresh fatty tissue, butter was chosen to act as the phantom material for human fat tissue.

F. The Low Frequency Refractive Index Spike

From the spectroscopy results obtained while developing emulsion phantoms for invasive ductal carcinoma and fibrous tissue, it was noticed that the refractive index of the emulsion-based phantoms appeared to spike around 0.3 THz. Since the reported refractive indices of the fresh breast tissues did not display such a rapid change in refractive index, the cause of the spike was investigated to determine if it could be removed or rectified.

To determine what part or parts of the phantom were contributing to the spike, the components used in the phantoms were individually characterized. As the water, oil and detergent are liquids, they were characterized using a liquid sample holder, described in section 2.A, to guarantee that the thickness of the liquid samples was both known and uniform. The TX151, however, was unable to be characterized using this method as it is normally in a powder form. To get the TX151 into a state where it was capable of undergoing THz spectroscopy, the powder was compressed into a tablet using five tons of pressure generated from a hydraulic press. Since the tablet's thickness was consistent and could be accurately measured with a micrometer, the spectroscopy results could be used to determine the properties of the TX151 tablet.

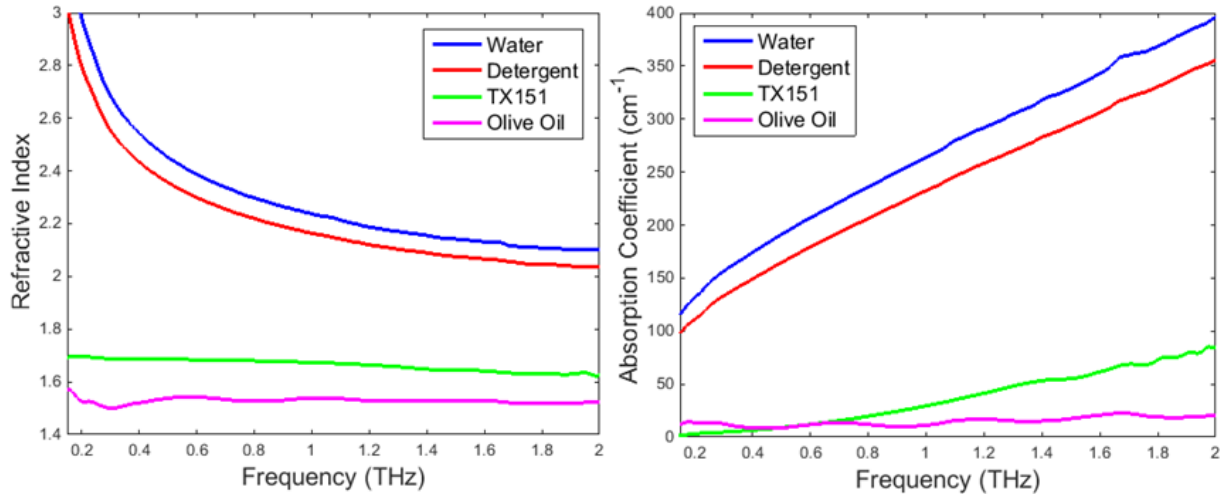

Figure 2.13. The refractive index and absorption coefficient of the component ingredients of the emulsion-based phantoms.

The resulting refractive index and absorption coefficient of four components can be found in figure 2.13. As can be seen from the figure, both the water and the neutral detergent exhibited the same sort of low frequency refractive index spike as the phantoms while neither the TX151 nor the olive oil showed similar behavior. As a major component in the detergent is water, it was determined that the major cause of the low frequency refractive index spike was the water. Unfortunately, since water is not only the main component of the phantoms but also required to react with the TX151 for solidification, it cannot be replaced without completely retooling the makeup of the phantoms.

G. Extending the Usable Lifetime of the Phantoms

While the TX151 emulsion phantoms are able to reliably mimic the optical properties of their respective fresh breast tissue, the amount of time that a given phantom can maintain its optical properties is relatively short. As seen in figure 2.14, after sitting out in the open air for twenty-four hours, both the refractive index and absorption coefficient of a fibrous tissue phantom decrease dramatically. This decrease in both optical properties is indicative of a lower percentage of water in the phantom, most likely due to evaporative water loss.

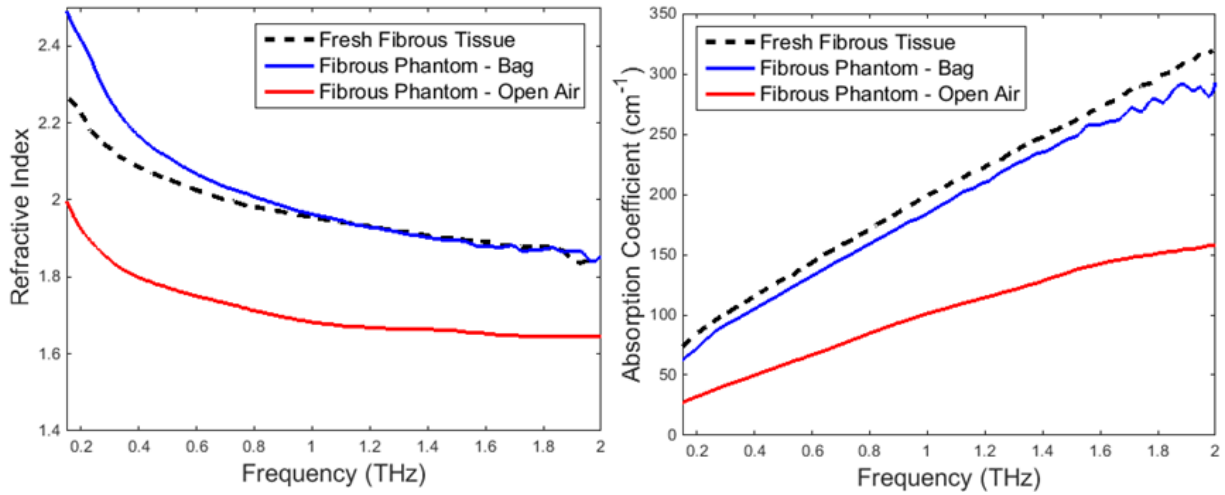

Figure 2.14. The refractive index and absorption coefficient of fibrous breast tissue phantoms stored in either a sealed bag or open air for 24 hours compared to freshly excised fibrous breast tissue [8].

In an attempt to curb the loss of water, the effects of storing the phantom in a sealed plastic bag were tested. This was done by making a new fibrous tissue phantom, cutting it in half and storing one half of the phantom in a sealed bag and the other half in the open air for twenty-four hours. After the twenty-four hours, each half of phantom was characterized using THz time-domain spectroscopy. As can be seen in figure 2.14, the half of the phantom stored in the sealed plastic bag maintained optical properties similar to fresh fibrous breast tissue while the half stored in the open air had a large reduction in both its refractive index and absorption coefficient. Unfortunately, while a simple method of storage was found that could slow the degradation of the phantoms, the phantoms would have to be removed from the bag for extended periods of time to be utilized as imaging phantoms. To minimize the losses to exposure, alterations to the composition of the phantoms were explored. The first such alteration that was tested was an inclusion of bleach. Three fibrous tissue phantoms were made with either 1, 5 or 10mL of bleach. To roughly maintain the optical properties of the phantom, as bleach has a relatively high refractive index and absorption coefficient, the addition of bleach was coupled with a one-to-one reduction in the amount of water used in the phantom. The three phantoms immediately

underwent THz spectroscopy after being made to get a baseline for their optical properties. They were then left out in open air for twenty-four hours before being characterized a second time.

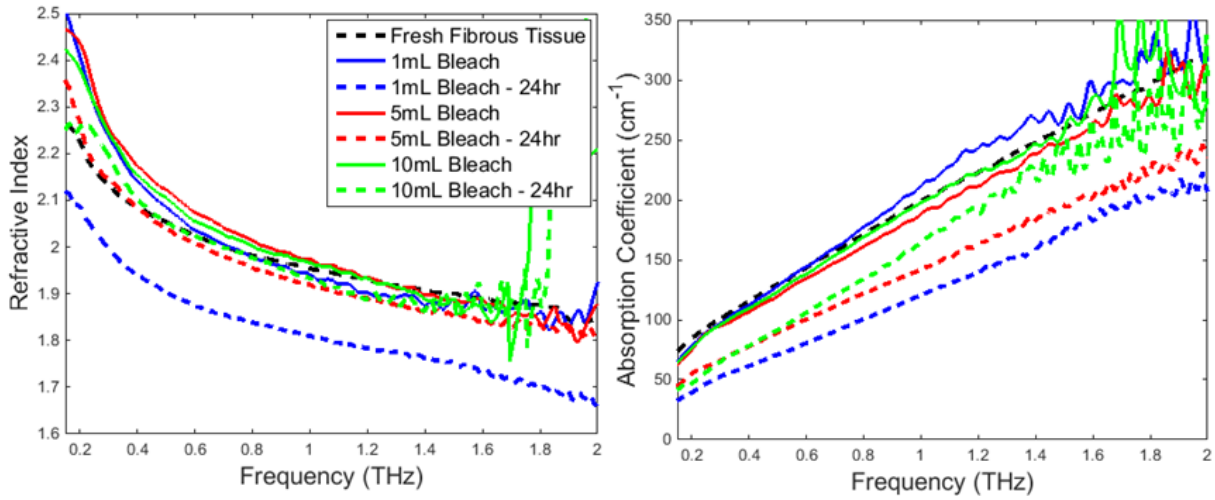

Figure 2.14. The refractive index and absorption coefficient of fibrous breast tissue phantoms with additions of bleach before and after being stored in open air for 24 hours compared to freshly excised fibrous breast tissue [8].

As can be seen in figure 2.14, the replacement of water with bleach had little immediate effect on the optical properties of the phantoms while also having a positive impact on the lifetime of the phantoms. The 5 and 10mL additions of bleach resulted in phantoms that maintained their refractive index even after twenty-four hours of exposure. Also, while the addition of bleach was unable to completely preserve the absorption coefficient, better preservation was observed as the amount of bleach used increased.

Unfortunately, adding bleach into the phantoms had some unforeseen consequences. The first consequence was that as more water was replaced by bleach the longer the phantom took to solidify. Typically, a fibrous tissue phantom with no bleach takes around five minutes to completely solidify while a phantom with a 10mL bleach replacement takes almost forty minutes, an almost eight-times increase. Additionally, while the phantom with 10mL of bleach best preserved its optical properties, it was also the most physically unstable making it difficult

to work with. Due to the incomplete preservation of the absorption coefficient and the other consequences causing bleach to be an imperfect solution, other additives were explored.

The next additive that was tested was guar gum. Guar gum is a plant derived polysaccharide that tends to increase the viscosity of water and stabilize emulsions. To determine if these properties would help prevent the degradation of the optical properties of the emulsion phantoms over time, four fibrous tissue phantoms were made with either a 1, 2, 3 or 4g addition of guar gum. After being made, half of each phantom was stored in a sealed bag while the other half was left exposed. Unfortunately, the strong thickening capabilities of the guar coupled with the solidification of the TX151 prevented the compositions with either 3 or 4g additions of guar from fully blending together which resulted in localized spots with more guar than others. Thus, to accurately determine the effects of the higher levels of guar, two new phantoms were made with either 3 or 4g of guar. However, the amount of guar used in these new phantoms was matched with an equal decrease in TX151.

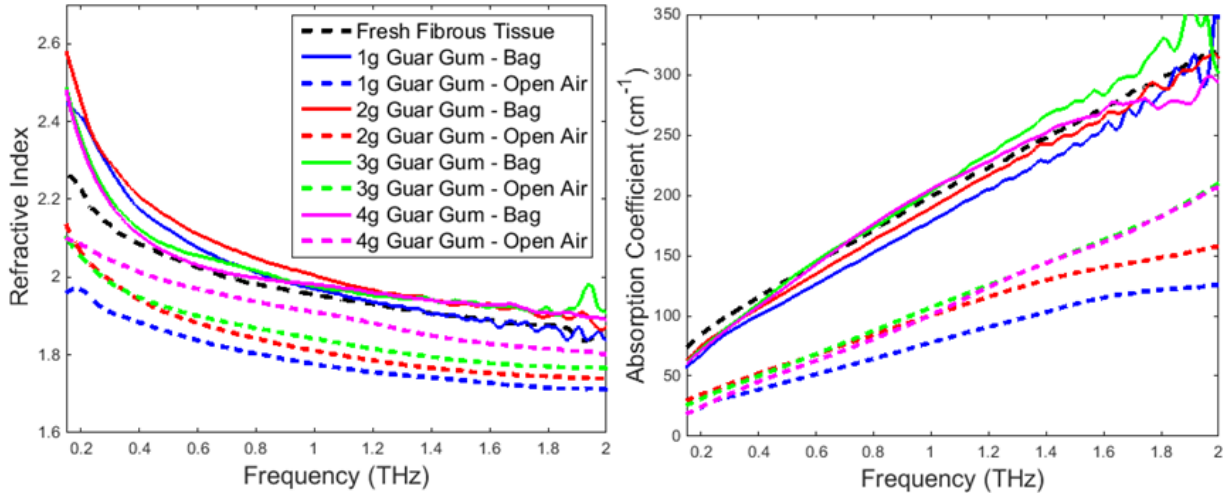

Figure 2.15. The refractive index and absorption coefficient of fibrous breast tissue phantoms with additions of guar gum stored in either a sealed bag or open air for 24 hours compared to freshly excised fibrous breast tissue [8].

After twenty-four hours, both halves of each of phantoms underwent THz time-domain spectroscopy to obtain their optical properties. As seen in figure 2.15, the more guar gum that

was used in the phantom, the better the refractive index of the half of the phantom exposed to open air was preserved. Unfortunately, like with the bleach, no such trend was observed for the absorption coefficient. But, unlike bleach, guar gum caused no extraneous complications to the phantoms it was included in.

Since neither of the previously tested additives could prevent the drop in absorption coefficient over time, a third additive, agar, was tested. Agar, like guar gum, is a plant-derived polysaccharide tends to form a gel-like material when mixed with water. To determine the effect that agar has on the effective lifetime of the emulsion phantoms, four fibrous tissue phantoms containing either 1, 2, 3 or 4g of agar were made after which half was stored in sealed plastic bags while the other half was left exposed to open air. After twenty-four hours, each half was characterized and the resulting optical properties where compared against each other. From this comparison, it was found that as the amount of agar used in the phantom increased the preservation of both the refractive index and absorption coefficient for the exposed half of the phantoms improved. To see if this trend would continue for greater amounts of agar, the same procedure was followed for fibrous tissue phantoms containing 5, 6 and 7g of agar. As can be seen in figure 2.16, the fibrous phantom containing 7g of agar could maintain a refractive index and absorption coefficient similar to that of fresh fibrous breast tissue despite being exposed to open air for twenty-four hours. Since any given phantom will most likely not need to be out of a bag for more than twenty-four hours, the addition of agar was chosen to be included in all future emulsion phantoms.

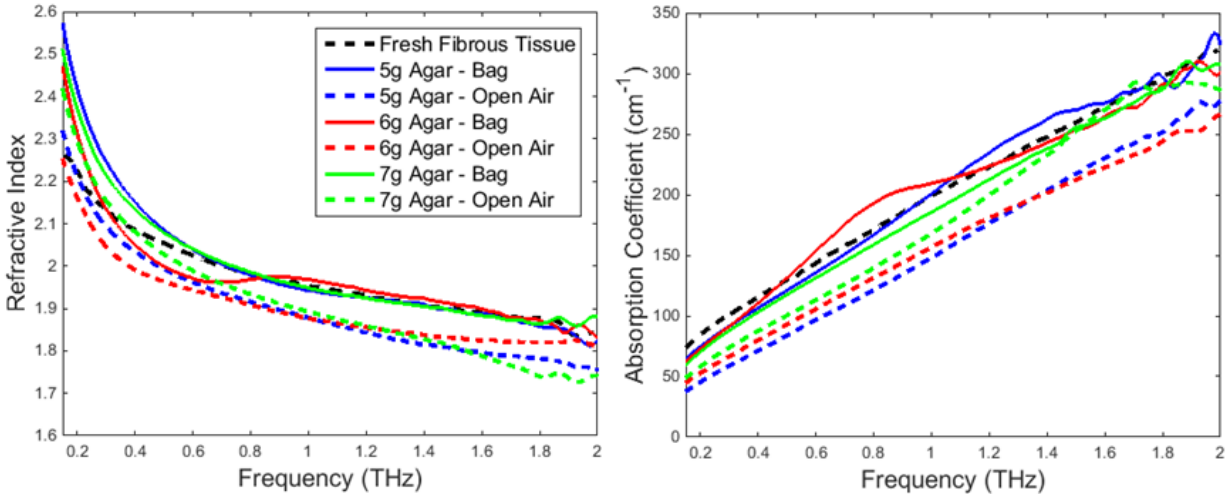

Figure 2.16. The refractive index and absorption coefficient of fibrous breast tissue phantoms with additions of agar stored in either a sealed bag or open air for 24 hours compared to freshly excised fibrous breast tissue [8].

III. Microdiamonds and Onion-Like Carbon as Contrast Agents for Terahertz Imaging

Previous work on terahertz (THz) imaging of breast cancer tumors has shown that it is possible to distinguish between cancerous tissue and healthy breast tissue [6], [7]. This ability is mainly due to the differences in electrical properties between the healthy fibrous and fatty breast tissue and cancerous tissue like invasive ductal carcinoma (IDC) [8]. While the difference between fatty tissue and cancerous tissue is readily apparent, the properties of fibrous breast tissue and IDC are relatively similar. This similarity between healthy fibrous tissue and cancerous tissue can lead to difficulty in distinguishing between adjacent regions of fibrous and cancerous tissue which could lead to incorrectly characterized tumor margins.

One method that could be used reduce this difficulty would be to utilize a contrast agent. If a contrast agent could be localized to the region of cancerous tissue, the relative difference in optical properties between fibrous tissue and IDC could be increased which would lead to an increase in the ability of THz imaging to distinguish between healthy and diseased tissue. The family of contrast agents chosen to be explored for their viability in THz imaging is nanometer and micrometer scale carbon particles as they are commonly used in optical imaging as contrast and fluorescence agents.

Carbon-based particles are available in a large variety of sizes, treatments and subtypes. More specifically, most carbon-based particles used as contrast agents tend to either be high pressure, high temperature synthetic diamond or onion-like carbon (OLC). While OLC typically has sizes on the order of nanometers, diamond particles with sizes in both the nanometer and micrometer range can be used. Additionally, diamond particles can be subjected to two different treatment types which alter their crystal lattice structure. The first treatment is to take pristine diamonds and irradiate them to make irradiated (Irr) diamonds. This process causes carbon atoms to be

knocked out of the crystal lattice resulting in vacancies. The second treatment involves taking the Irr diamonds and annealing them at high temperatures to form irradiated-annealed (Irr-Ann) diamonds. The annealing allows non-carbon atoms to fill the vacancies converting them into color centers. These two treatments are typically used to create diamond particles that fluoresce at a specific frequency.

To narrow down the wide selection of options, some preliminary work had already been performed using samples of PDMS containing a known concentration of one of six particles whose subtype, size and treatment were known. The particles that were tested included 100nm OLC, 40nm pristine diamond, 100nm pristine diamond, 100um pristine diamond, 150um Irr diamond and 150um Irr-Ann diamond. The optical properties of each of the samples were obtained by performing transmission THz time-domain spectroscopy with a TPS Spectra 3000. The resultant optical properties for the nanometer-scale particles and the micrometer-scale particles were compared to the properties of a pure PDMS sample to determine what effect, if any, the addition of particles had on the optical properties of the samples.

For the nanometer-scale particles, it was found that the additions of 40nm and 100nm pristine diamonds provided little to no increase in either the refractive index or absorption coefficient as compared to pure PDMS. The 100nm OLC, on the other hand, provided a relatively uniform increase in both the refractive index and absorption coefficient. For the micrometer-scale particles, it was found that all three of the tested diamonds provided a resonance like behavior to the absorption coefficient with the 100um diamond particles providing the strongest increase. While the two 150um diamonds caused weaker resonance-like behavior, there is a clear difference between the magnitude of the two treatments with the IrrAnn diamonds providing the

strongest response. This suggests that diamonds with different treatments may have different responses in the THz band.

From these results, it was determined that the primary focus of this work would be on micrometer-scale diamonds and nanometer-scale OLC. In order to determine which particle from these two groups would act as the best THz imaging contrast agent, two different sizes of OLC and five different sizes of diamonds, each with at least two different treatment types, were acquired from Adámas Nanotechnologies [19].

A. Characterization of Microdiamonds in Polyethylene

Micrometer-scale diamonds have two main forms of variation: their size and what sort of treatment, if any, they had undergone. In order to determine what effects these variation shave on the THz optical properties of the diamonds and whether a specific combination would make for an effective THz contrast agent, thirteen different diamond particles were obtained from Adámas Nanotechnologies [19]. This set of particles included 150um Irr and IrrAnn diamonds, 100um pristine and Irr diamonds, 40um pristine, Irr and IrrAnn diamond, 20um pristine, Irr and IrrAnn diamonds and 1um pristine, Irr and IrrAnn diamonds.

The first set of diamond particles that were tested were the 100um pristine diamonds as they had the best results of the microdiamonds from the preliminary tests. Unlike the preliminary tests however, the diamond particles were not embedded in PDMS. This was because, due to their relative heaviness, diamonds particles with micrometer-scale diameters are unable to be distributed throughout the PDMS and are instead forced to exist in a monolayer. Instead, the powdered polyethylene was chosen to act as the background medium. The diamond particles would be mixed into the polyethylene before being pressed into a solid tablet. The tablet is formed by utilizing a hydraulic press to apply 5 tons of pressure to the mixture of diamond

particles and polyethylene. As polyethylene is extremely transparent in the THz band, any minor changes in either the refractive index or absorption coefficient can be detected.

The first particle type that was incorporated into the polyethylene and tested was the 100um pristine diamond. This was done as the resulting optical properties could be compared to those of the PDMS sample. For a better comparison, the tablet was made such that the weight concentration of diamond particles was the same as the PDMS sample, 10 wt.%. This was achieved by using 180mg of polyethylene and 20mg of the pristine 100um diamond. The optical properties of the tablet were obtained by performing transmission THz time-domain spectroscopy and where compared to the properties of a tablet made of pure polyethylene.

While the increase in refractive index for the tablet (figure 3.3) was similar to the increase observed in the PDMS, the resonance-like behavior in the polyethylene tablet was diminished and broadened when compared to the behavior observed in the PDMS. The main theory to explain this difference was that a major contribution to the increase seen in the absorption coefficient is due to scattering of the signal by the particles and not form actual absorption. If this theory is true, then the differences observed in the absorption coefficient would be mainly due to difference in the pattern of distribution between the PDMS (monolayer) and the polyethylene tablet (dispersed).

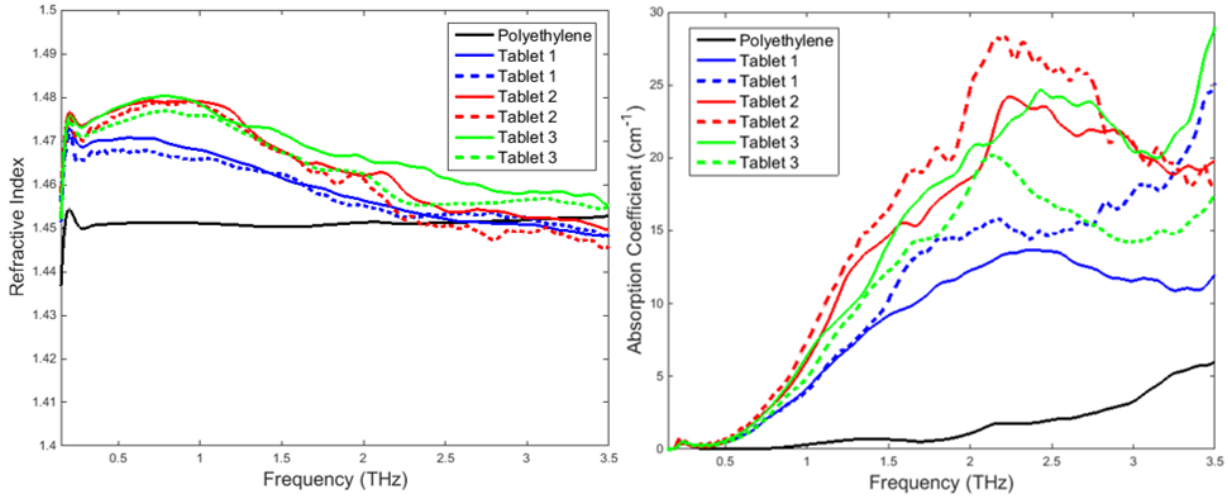

Figure 3.1. The refractive index and absorption coefficient of three polyethylene tablets that contain 10 wt.% of pristine 100um diamond. Solid and dotted lines represent a 90 degree difference in the measurement orientation.

To determine how much scattering was influencing the measured absorption coefficient, two steps were taken. The first step was that two new tablets were made, both with a 10 wt.% addition of 100um pristine diamond particles. The second step entailed characterizing the original tablet a second time after being rotated 90 degrees as well as charactering the two new tablets at two orientations 90 degrees apart. From these results (figure 3.3) it can be seen that while there is little difference between all of the refractive indices, the absorption coefficients exhibit strong amounts of variance. Not only are there strong variations between different tablets despite having the same amount and type of diamond particles, there is also non-negligible variations present within a tablet when characterized at different orientations. These differences suggest that each tablet has a unique distribution of particles at the site of spectroscopy and thus the THz signal will interact with a different number of particles as it travels through the tablet and thus the amount of scattering caused by the tablet will be different. Additionally, the scattering is dependent on the orientation of the particles themselves with respect to incident THz signal such that by rotating the sample the amount of scattered signal that happens to reach the receiver changes.

In order to gain a better understanding of the actual diamond properties, each of the three tablets were broken down and reformed three times. For each iteration, the tablet was characterized twice at two different orientations 90 degrees apart. Then, for each tablet, the eight sets of optical properties were averaged together and compared to each other. As can be seen from figure 3.4, the average absorption coefficient for each of the tablets are relative similar to one another. Thus, while the averaging process doesn't completely remove the effects of scattering from the absorption coefficient, it can provide an estimate for the average change an addition of 100um pristine particles would cause.

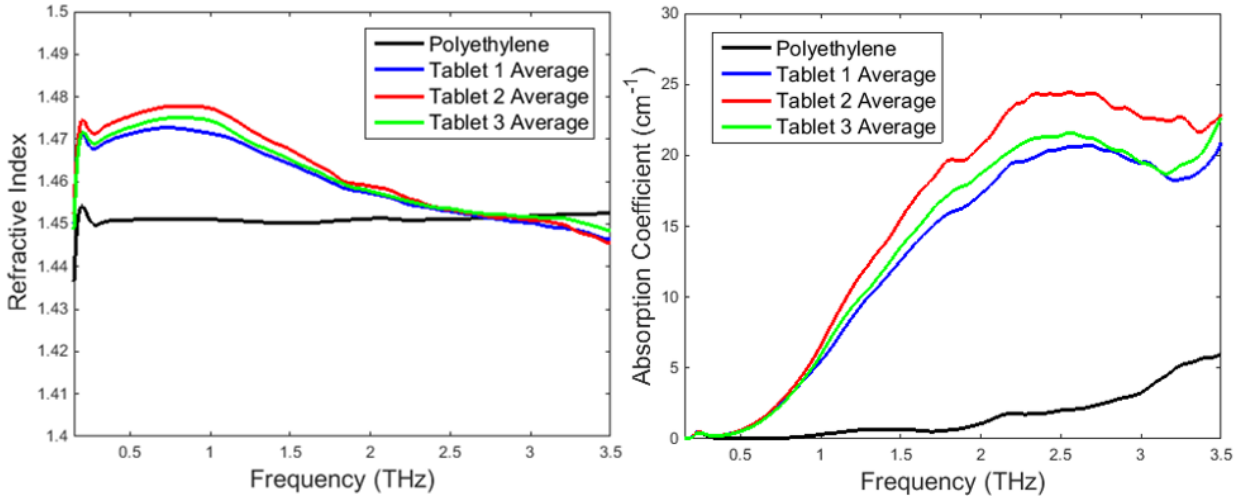

Figure 3.2. The average refractive index and absorption coefficient for three polyethylene tablets that contain 10 wt.% of pristine 100um diamond.

With the effects of the 100um pristine diamond particles relatively well known, previously untested diamond particles were used to determine if any of them would work better as a THz contrast agent. The first particle that was chosen was the 40um pristine diamond as it would help determine what effects reducing the size of the particle would have on the resulting optical properties. To be able to compare the results with those of the 100um pristine diamonds, three polyethylene tablets were made using 180mg of polyethylene and 20mg of 40um pristine diamonds so that there was a 10 wt.% concentration of particles. Each of the three tablets were

characterized at two orientations 90 degrees apart before being broken down and reformed. This process was repeated twice such that each tablet had been characterized a total of six times. Figure 3.5 shows all of the measured refractive indices and absorption coefficients for one the tablets. These results show that the variation between orientations and iterations are much less than what was observed for the 100um pristine diamond tablets. This was expected as the 40um particles, when compared to the 100um particles, are electrically small and would thus cause less scattering. The smaller size may also be the reason that no peak was observed in the absorption coefficient for the tablets containing 40um pristine diamond. For the 100um particles, the peak was around 3THz which happens to have a wavelength of100um. If this behavior is assumed to be true for all particle sizes, then the peak caused by the 40um particles would be around 7.5THz which is outside the observable range of the TPS Spectra 3000 used to take the measurements.

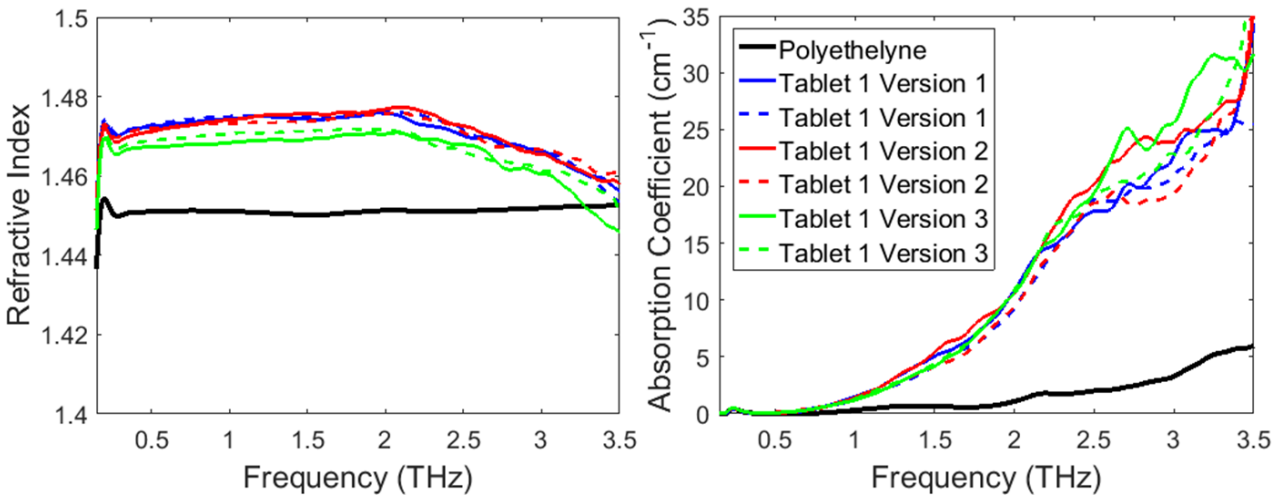

Figure 3.3. The refractive index and absorption coefficient for three iterations of a polyethylene tablet that contains 10 wt.% of pristine 40um diamond. Solid and dotted lines represent a 90 degree difference in the measurement orientation.

All of the measurements taken from tablets made with 40um pristine diamond particles were averaged together to determine the average expected effects (figure 3.6). When compared to the results of the 100um diamond tablets, the tablets with 40um pristine diamond particles provided a greater increase in refractive index at all frequency above 1THz. However, the increase in the

absorption coefficient for the 40um particles was lower than the increase provided by the 100um particles at all frequencies below 3THz.

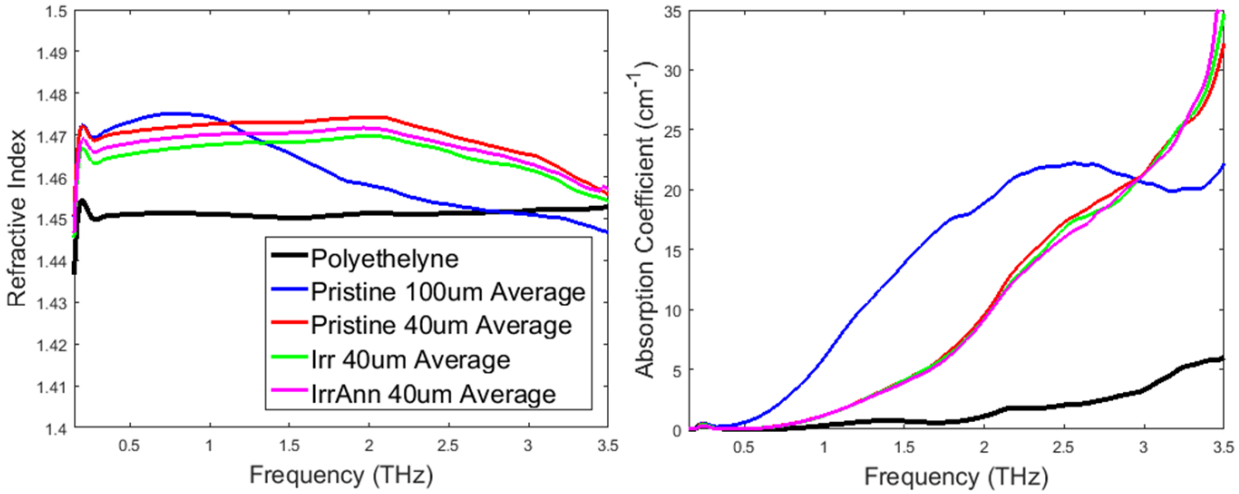

Figure 3.4. The average refractive index and absorption coefficient for polyethylene tablets that contain 10 wt.% of either pristine 100um diamond, pristine 40um diamond, Irr 40um diamond or IrrAnn 40um diamond.

As the 40um particle size was the first size particle used for which all treatment types were available, it was chosen to determine what effects, if any, the different treatment types provided. Like for the previously tested particles, the Irr and IrrAnn 40um diamond particles were each incorporated into three different tablets made of 180mg of polyethylene and 20mg of the diamonds in order to achieve a 10 wt.% concentration of particles. Each of the tablets underwent transmission THz time-domain spectroscopy at two orientations 90 degrees apart after which they were broken down and reformed, and characterized again. The results for all of the measurements were averaged together and compared to average optical properties of the tablets with 40um pristine diamond. As can be seen in figure 3.6, both the Irr and IrrAnn 40um diamonds provided increases in the refractive index and absorption coefficient that did not vary from the increase provided by the pristine version. This shows that the different treatment options have little to no effect on the resulting optical properties in the terahertz band. This

allowed future work to focus on the cheaper and more readily available pristine versions of the diamond particles.

To round out the effects that the size of the diamond particles has on the resulting optical properties, the 20um and 1um pristine diamond particles were tested. This was done by incorporating each of the two particle types into three tablets made of 180mg of polyethylene and 20mg of diamond. Each of the tablets were characterized at two orientations 90 degrees apart. The measured optical properties were then averaged together and compared to the averages of the 100um and 40um diamond particles.

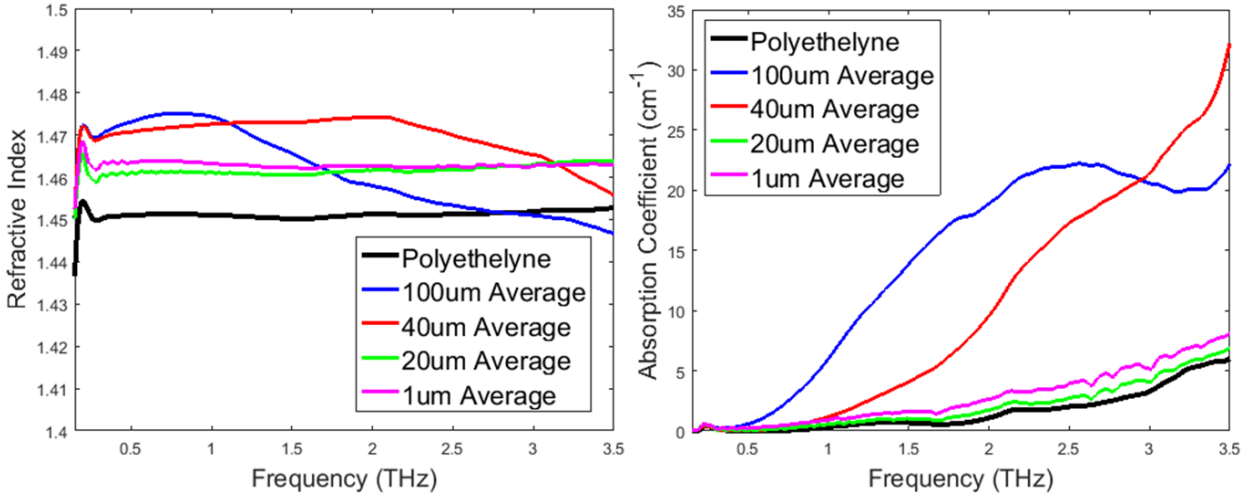

Figure 3.5. The average refractive index and absorption coefficient for polyethylene tablets that contain 10 wt.% of either pristine 100um diamond, 40um diamond, 20um diamond or 1um diamond.

As can be seen in figure 3.7, the increases in the refractive index and absorption coefficient from the addition of both the 20um and 1um pristine diamond particles were much less than the increases provided by the larger particles. Additionally, both the 20um and 1um particles provided nearly identical increases in both optical properties. This lead to concerns that one of the particles used was not the size that it was believed to be.

To test to see if this was true, particles at these sizes but with different treatments were tested by being incorporated into polyethylene tablets using the same procedure as was used for the other

particles. As the different treatments were previously shown to not provide significant changes to the resulting optical properties, if the pristine particles were not the sizes they were believed to be, there would be differences between properties of the pristine and treated particles. From figure 3.8, it can be seen that the measurements of the tablets with the 20um and 1um Irr and IrrAnn diamonds had refractive indices and absorption coefficients nearly identical to the tablets containing the respective pristine versions.

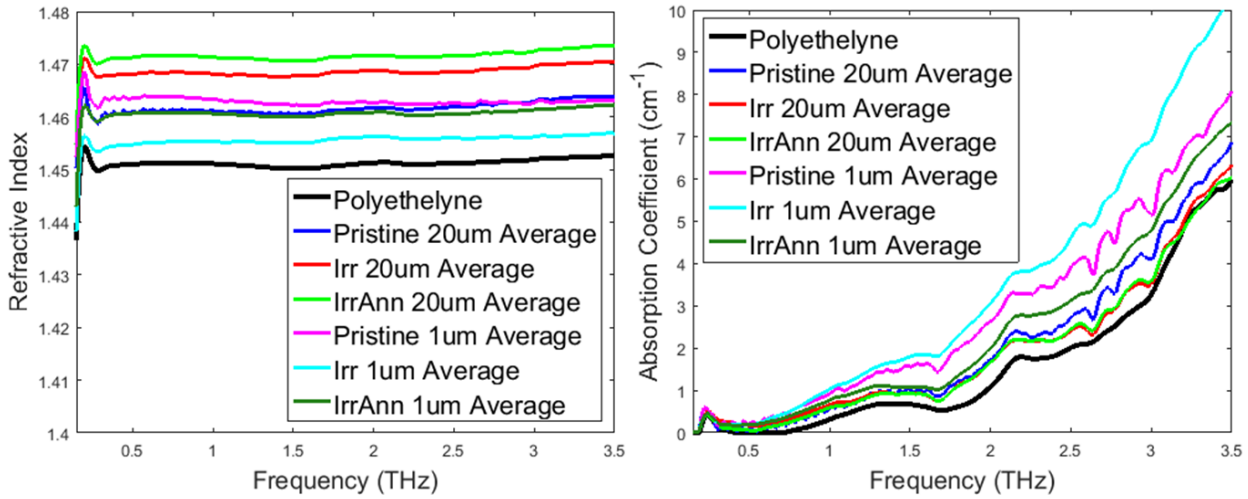

Figure 3.6. The average refractive index and absorption coefficient for polyethylene tablets that contain 10 wt.% of either pristine, Irr or IrrAnn 20um diamond or 1um diamond.

To further verify that the pristine particles used were of the sizes they were believed to be, optical microscopy at 400x magnification was used to image both the 20um and 1um pristine diamond particles. From the images seen in figure 3.9, there is clear difference in the size of the two particles which suggests that the similarities are due to the particles being below some sort of scattering threshold and that the larger increases from the larger particles are mostly due to scattering.

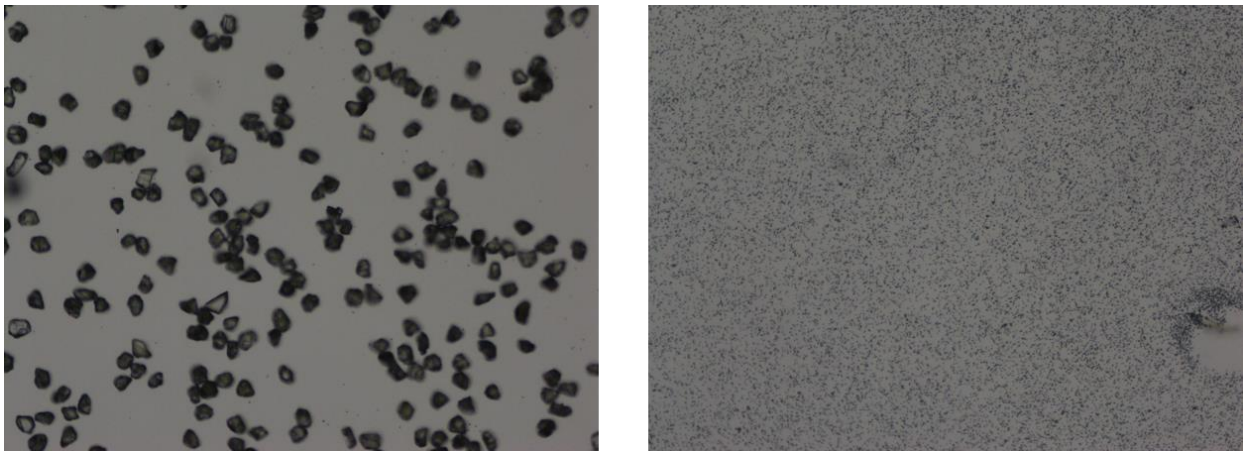

Figure 3.7. Optical microscopy images at 400x magnification of pristine 20um diamonds (left) and pristine 1um diamonds (right).

In conclusion, it was found that for the micrometer-scale diamond particles, the size of the particle is the main influence on the resulting refractive index and absorption coefficient. Specifically, as the size decreases, the location of the resonance-like peak in the absorption coefficient moves to higher frequency and once the size of the diamonds reach at least 20um, the amount of scattering induced by the particles becomes negligible. Additionally, it was found that neither the Irr or IrrAnn diamonds provided a different change in optical properties than their pristine counterparts. Overall, it was found that the 100um pristine diamond particles would act as the best THz contrast agent out of all the micrometer-scale diamonds.

B. Characterization of Onion-Like Carbon in Polyethylene

To determine whether if the OLC would act as a better contract agent for THz imaging than the micrometer-scale diamonds, the 100nm OLC was incorporated into polyethylene tablets. A set of two polyethylene tablets with a 1 wt.% concentration of 100nm OLC were made to match the concentration used in the PDMS sample used in the initial testing. This was done by using 198mg of polyethylene and 2mg of 100nm OLC. Each of the tablets were then characterized at two orientations 90 degrees apart. Each of the measurements were averaged together and compared to the average optical properties of the tablets with 10 wt.% of 100um pristine

diamond (figure 3.10). This comparison showed that a 1 wt.% addition of 100nm OLC could provide refractive index and absorption coefficient increase comparable to those provided by the 10 wt.% additions of micrometer-scale diamonds.

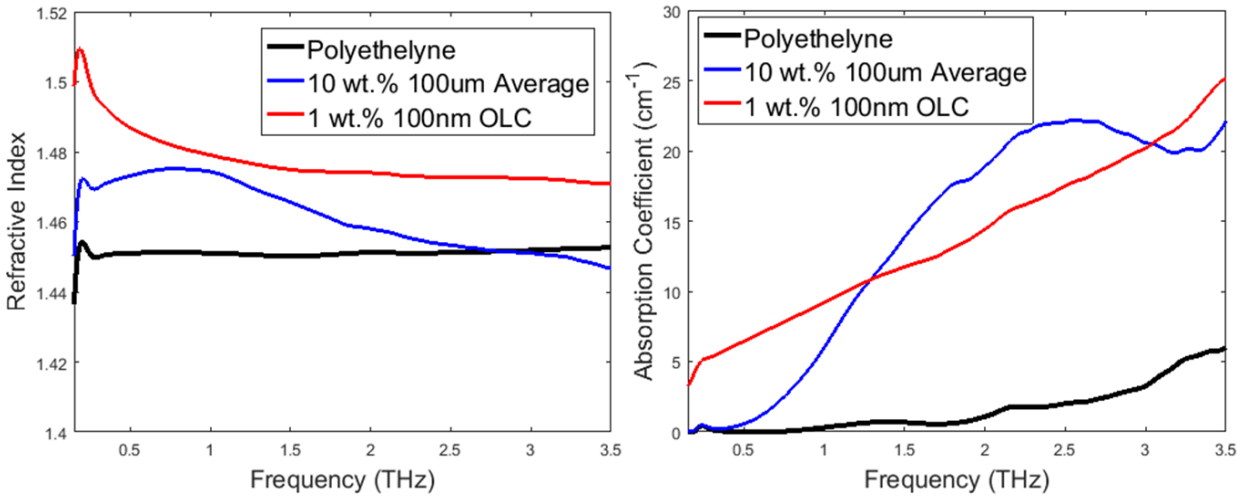

Figure 3.8. The average refractive index and absorption coefficient for polyethylene tablets that contain either 10 wt.% of pristine 100um diamond or 1 wt.% of 100nm OLC.

To better compare the effects of 100nm OLC versus the 100um diamond, two new tablets were made with a 10 wt.% concentration of the OLC by using 180mg of polyethylene and 20mg of the particles. However, after attempting to characterize the first tablet, it was found that the absorption of the tablet was too high and the tablet too thick to allow a measurable THz signal to penetrate through the tablet. To reduce then thickness of the tablet, the two 10 wt.% tablets were broken down and mixed together. The mixture of the two tablets was then used to make three new tablets with an effective thickness of two-thirds of the originals.

As a measurable signal was able to pass through these tablets, each tablet was characterized at two orientations 90 degrees apart. After characterization, the tablets were broken down and mixed together before three new tablets were made. After repeating the characterization on the new tablets, the resulting optical properties were averaged together and compared to the average properties of the tablets with a 1 wt.% addition of 100nm OLC and the tablets with the 10 wt.%

addition of 100um pristine diamond particles. From this comparison (figure 3.11) it can be seen that the 10 wt.% addition 0f 100nm OLC provides a much larger increase in both the refractive index and absorption coefficient than the same concentration of the best micrometer-scaled diamond. This large increase indicated that the OLC has a strong potential to act as a contrast agent for THz imaging.

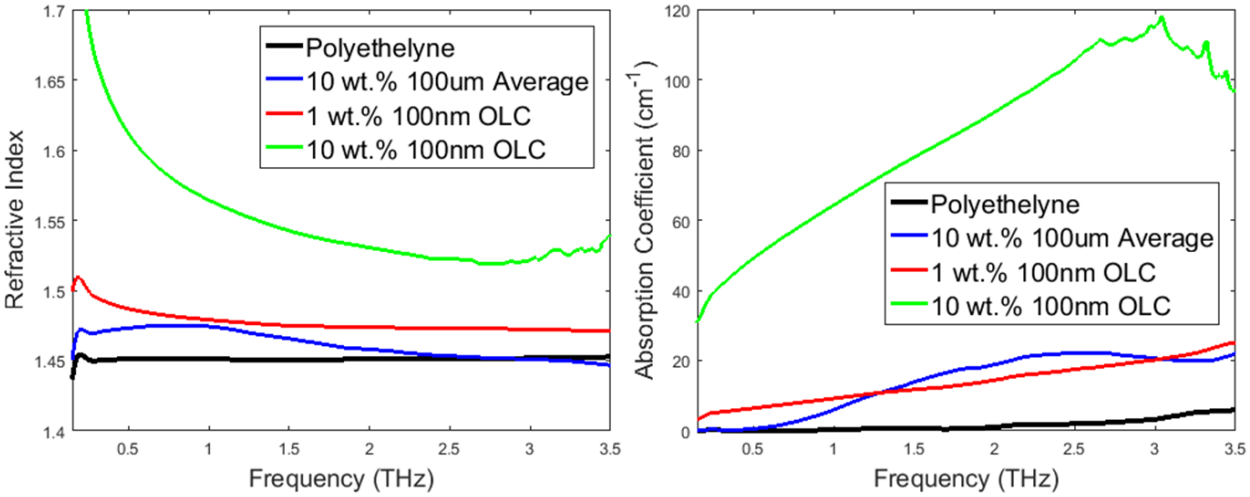

Figure 3.9. The average refractive index and absorption coefficient for polyethylene tablets that contain either 10 wt.% of pristine 100um diamond, 1 wt.% of 100nm OLC or 10 wt.% of 100nm OLC.

To see if the size of the OLC particles has an effect on the resulting optical properties, tablet with additions of 200nm OLC were made. To mimic the processes used for the 100nm OLC, two tablets were made with a 1 wt.% addition while another two were made with a 10 wt.% addition. The two tablets with the 10 wt.% addition were then broken down and mixed together before being remade into three tablets. Both sets of tablets were characterized at two different orientations 90 degrees apart before being broken down, reformed and characterized again. The results for each concentration of 200nm OLC were then averaged together and compared to the 100nm OLC tablets, as seen in figure 3.12. From this comparison it can be seen that the 200nm OLC provided a smaller increase in both refractive index and absorption coefficient than the 100nm OLC. This result indicated that not only is the 100nm OLC a better contrast agent than

the 200nm OLC but also that a trend that as the OLC gets smaller, the increase in optical properties provided by the same weight concentration, increases. Unfortunately, smaller OLC was unavailable for testing so the validity of this theory could not be tested further.

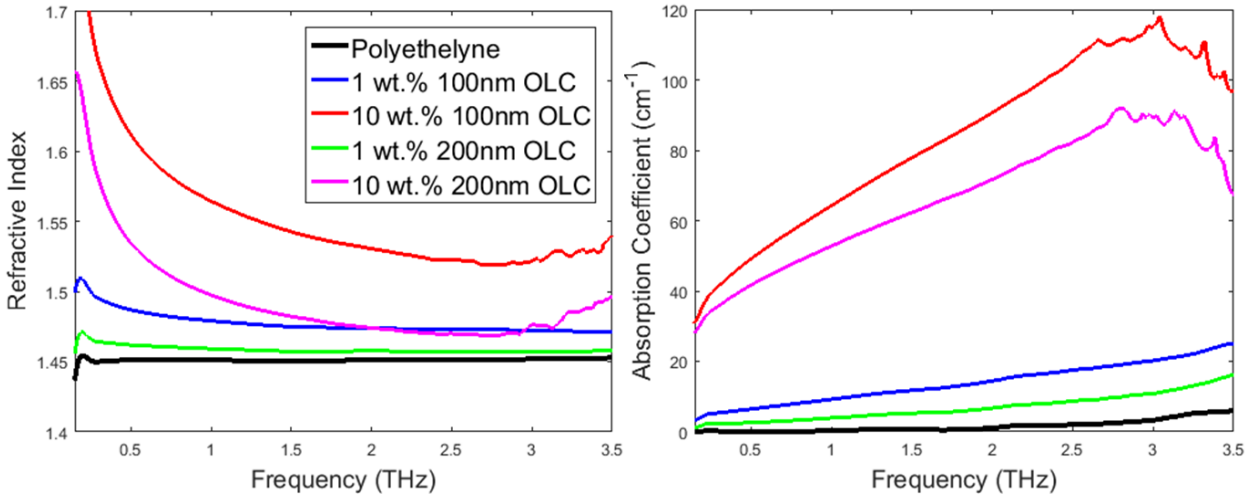

Figure 3.10. The average refractive index and absorption coefficient for polyethylene tablets that contain either 1 wt.% or 10 wt.% of either 100nm or 200nm OLC.

C. Enhanced IDC Phantoms

While the superiority of the 100nm OLC as a THz contrast agent over the 100um pristine diamond particles can be seen clearly from the results of the polyethylene tablets, polyethylene is highly lossless in the THz band. As the THz contrast agent would be used in the imaging of the highly lossy breast tissue, the effects of the potential contrast agents when in a lossy medium had to be determined. This was accomplished by utilizing the previously developed tissue phantom which mimics the optical properties of invasive ductal carcinoma (IDC) [16].

The first particle that was tested was the 100um pristine diamond. This particle was chosen as it acted the best contrast agent out of all the micrometer-scale diamond particles. To match the previous work in the tablets, a 10 wt.% addition of the microdiamonds was added into the phantom as it was being made. Once made, spectroscopy had to be performed on thin slices of the phantom as the high absorption of the phantom would prevent the transmission of the signal.

The first round of spectroscopy was performed on 200, 300, 400 and 500um thick slices using a liquid sample holder (see section 2.A). This range was chosen as the thicker slices would allow for the signal to interact with more of the particles while the thinner slices would allow more of the signal to pass through the sample which would increase the range of frequencies for which the optical properties could be determined. From the results of the spectroscopy, seen in figure 3.13, it can be seen that the addition of 100um pristine diamond caused a slight increase in the refractive index of the phantom while providing little to no increase in the absorption coefficient. Additionally, it was found that the even for the thinnest slice, the absorption of the phantom was too high to accurately determine the optical properties above 2.4 THz. This prevented any of the effects that the absorption peak caused by the 100um pristine diamonds from being observed. From these results, it was determined that, since the thinner slices didn't have a large difference from the thicker slices and because the absorption from the phantom in the thickest slices appeared to overpower any effects of the diamond particles, a 200um slice thickness would be used for all future phantom characterization.

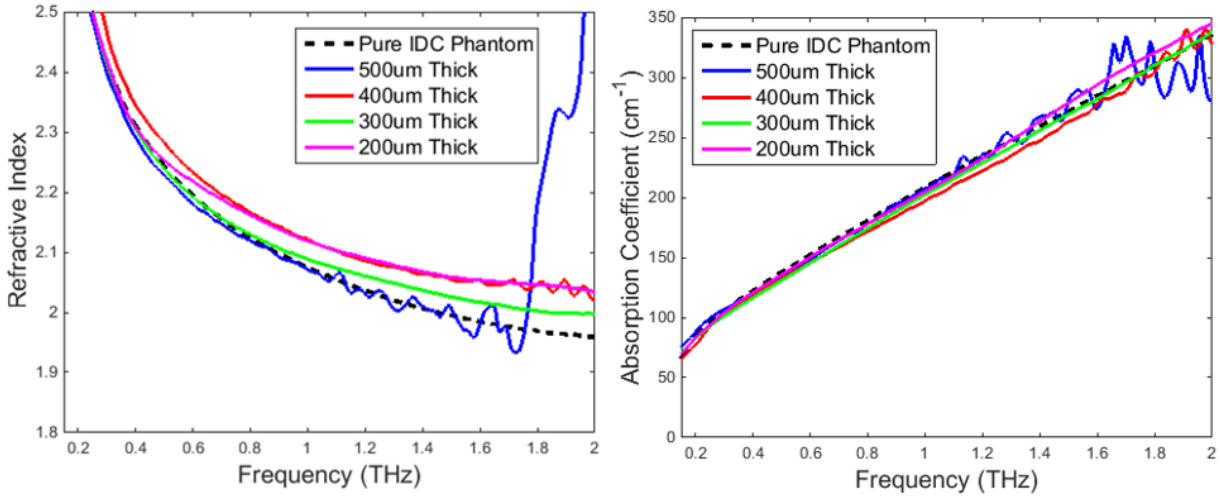

Figure 3.11. The refractive index and absorption coefficient of different thicknesses of IDC phantom that contains 10 wt.% of pristine 100um diamond compared to pure IDC phantom [16].

The second particle that was tested in the IDC phantom was the 100nm OLC as it was the best performing out of the two tested sizes of OLC. To start, two phantoms were made with a 1 wt.% addition of the OLC. Each phantom was characterized multiple times using different slices from the phantom. Due to size differences, the first phantom was characterized at six different locations while the second was characterized at nine. From these results, it was found that there was a relatively high variance in the refractive index between different locations in the same phantom. The mostly likely cause of this variance is that the addition of OLC unexpectedly quickened the solidification of the phantom which could have prevented the OLC from being evenly distributed. As this effect was known when making the second phantom, steps were taken to slow the solidification which would have allowed for a better distribution and thus less variance.

The measurements of the two phantoms together were averaged together and compared to the properties of pure IDC phantom and IDC phantom with a 10 wt.% concentration of 100um pristine diamond. As can be seen in figure 3.14, the one percent addition of 100nm OLC provided a greater increase in both the refractive index and absorption coefficient as compared to the addition of diamonds showing that even in a highly lossy medium like the IDC phantom, low quantities of 100nm OLC can act as a contrast agent.

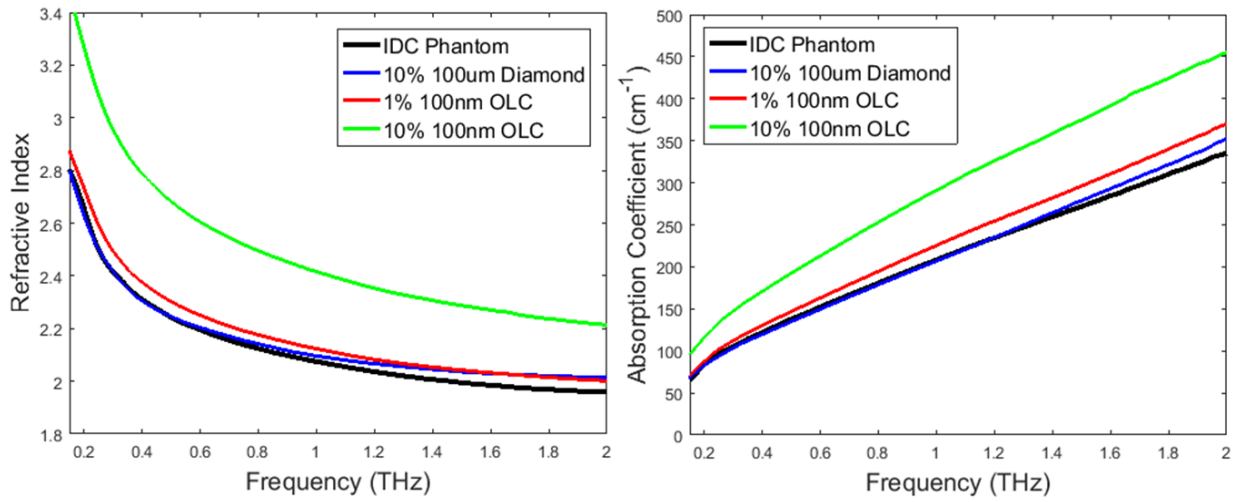

Figure 3.12. The average refractive index and absorption coefficient for IDC phantoms that contain either 10 wt.% of pristine 100um diamond, 1 wt.% of 100nm OLC or 10 wt.% of 100nm OLC [16].

However, the increase provided by the 1 wt.% addition was smaller than what was desired for an optimal THz imaging contrast agent. Thus, a phantom was made with a 10 wt.% addition of 100nm OLC to determine if the increase in concentration could still provide a stronger increase in optical properties. Only one phantom was made with this phantom due to the large amount of OLC required and the limited available supply. After being made, the phantom was characterized using eight different slices and the resulting optical properties were averaged together and compared to the average properties of the previously tested phantoms. (figure 3.14). As can be seen from the comparison, greater concentrations of OLC are still able to provide large increase in both the refractive index and absorption coefficient despite the naturally high properties of the phantom material.

As the 100nm OLC could provide such a large increase in the optical properties of the IDC phantom, it was chosen to be tested as a contrast agent. To determine if the OLC what effect the OLC would have if used in THz imaging of breast tumor margins, IDC phantoms containing 1 and 10 wt.% concentrations of 100nm OLC were imaged. Additionally, pure IDC phantom and fibrous tissue phantom were also imaged to act as comparisons to the enhanced IDC phantoms.

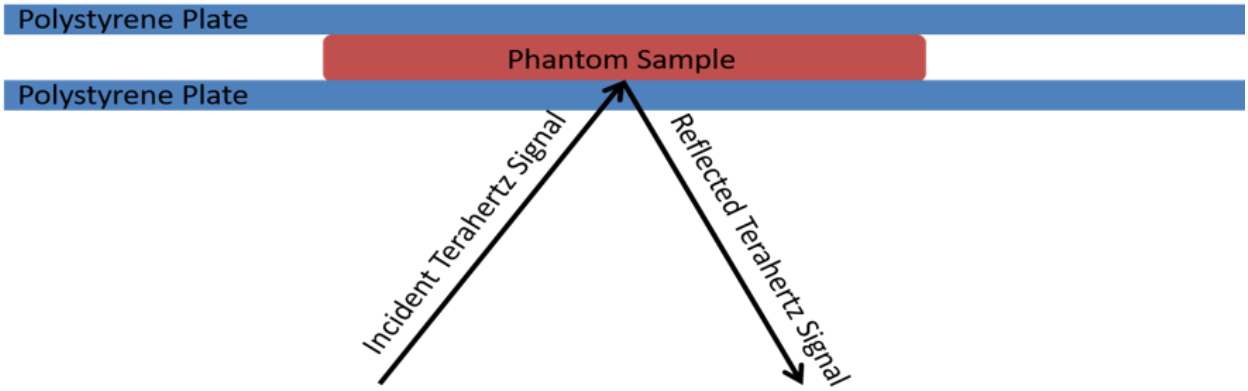

Figure 3.13. The initial setup used to perform THz imaging of phantom samples.

The first round of imaging was performed using the setup shown in figure 3.15. This setup involved having the phantom pressed between two polystyrene plates in an effort to create a flat imaging interface. After imaging each phantom, the images were compared as can be seen in figure 3.16. For each of the images, the colors represent the represents the maximum of the received reflected signal normalized to the reference measurement. From these images, it can be seen that there is a clear progression in measured signal strength with the fibrous phantom having the lowest, followed by the pure IDC phantom, the IDC phantom with 1 wt.% of OLC and the IDC phantom with 10 wt.% of OLC. This demonstrates that an addition of 100nm OLC is able to increase the amount of reflected THz signal and thus act as a contrast agent.

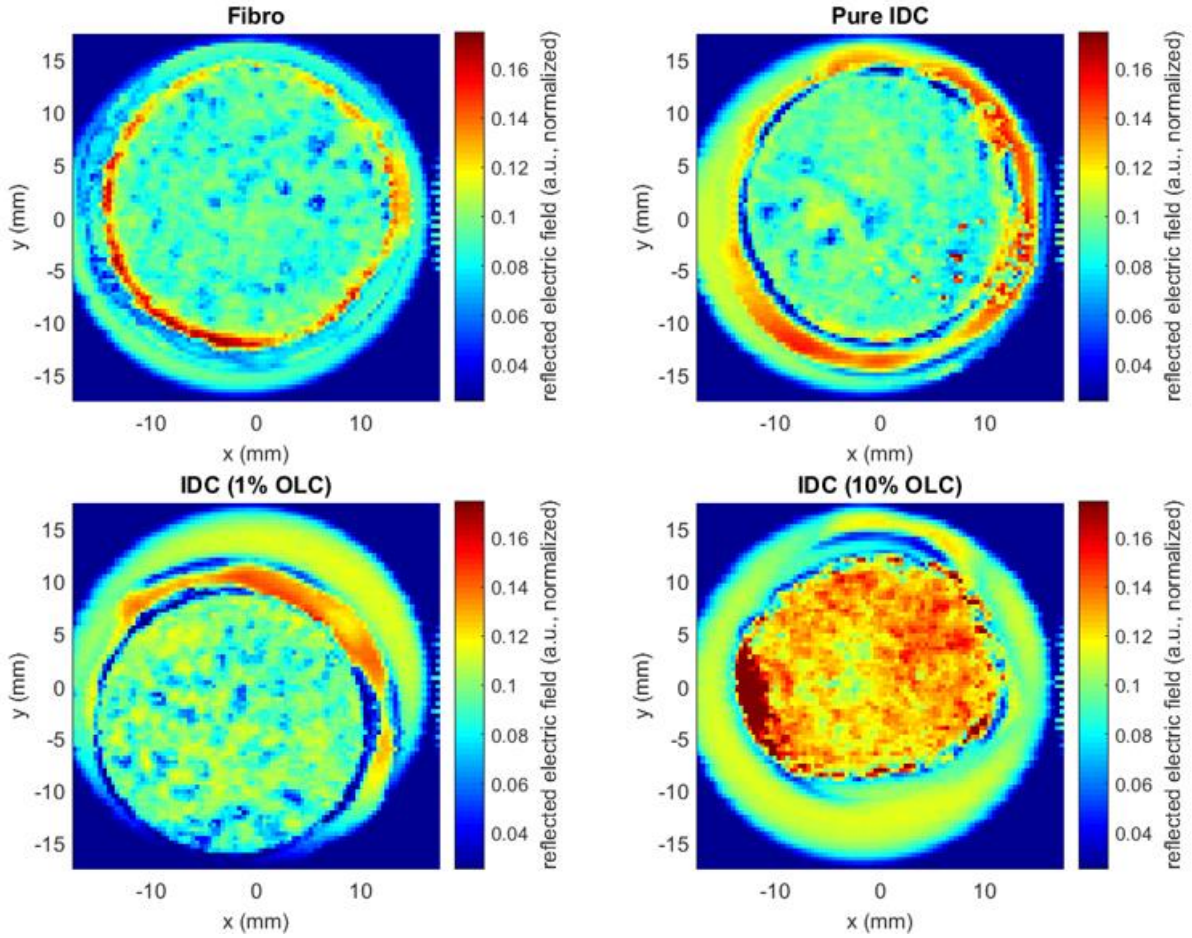

Figure 3.14. Terahertz images of the normalized, reflected electric field for fibrous phantom, pure IDC phantom, IDC phantom with 1 wt.% of 100nm OLC and IDC phantom with 10 wt.% of 100nm OLC utilizing the first imaging setup.

However, as seen in figure 3.16, each of the images of the phantom materials had a noise-like pattern of low measured signal. This was due to air gaps that formed between the polystyrene plate and the phantom. The air gaps were caused by the inherently rough surface of the phantom failing to adhere uniformly to the polystyrene plate despite the pressure exerted by the two plates on the phantom. In an attempt to resolve this issue, a second imaging setup was utilized. This setup removed the bottom polystyrene plate and directly imaged the phantom surface. As seen from figure 3.17, while the new imaging setup still showcased the same trend found using the original setup, it was unable to remove the effects of the roughness of phantom surface from the images.

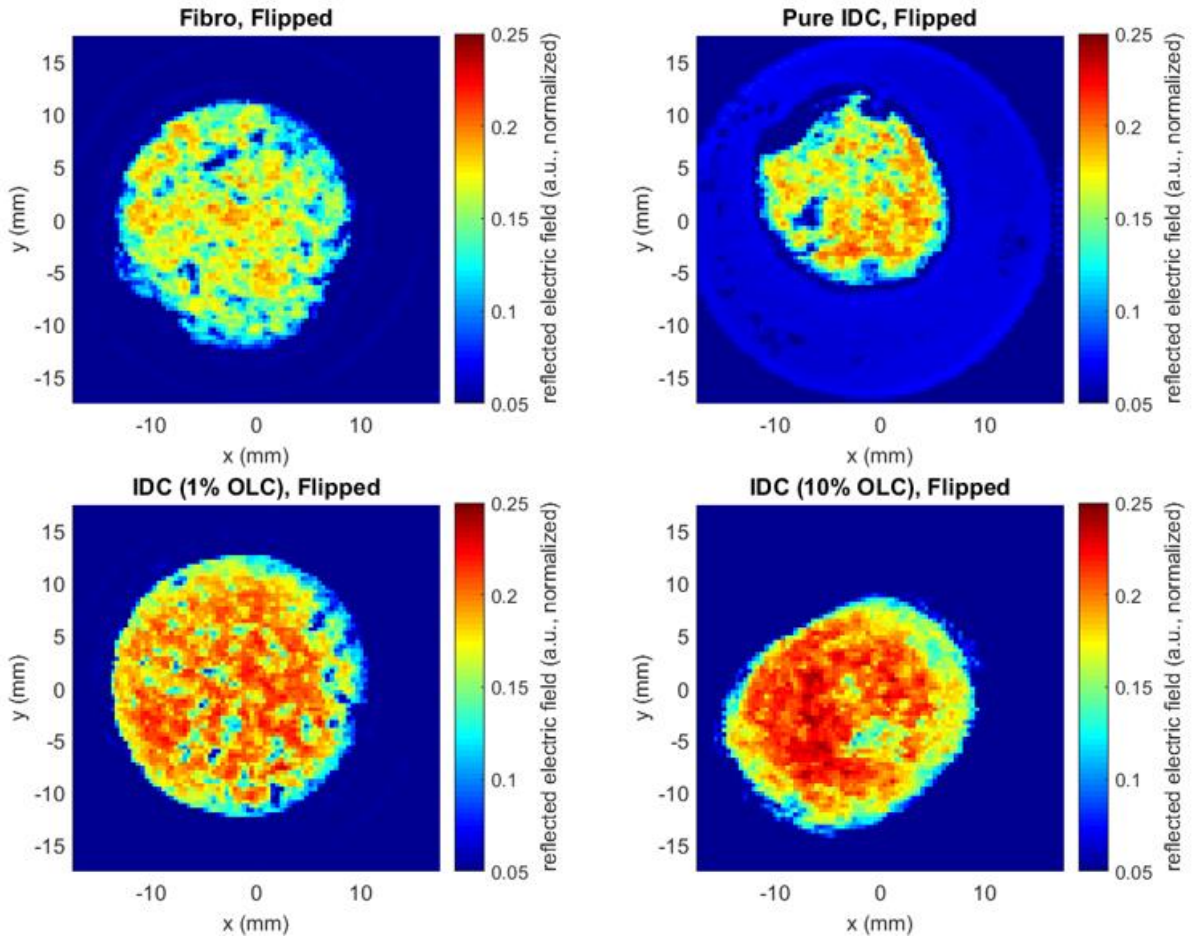

Figure 3.15. Terahertz images of the normalized, reflected electric field for fibrous phantom, pure IDC phantom, IDC phantom with 1 wt.% of 100nm OLC and IDC phantom with 10 wt.% of 100nm OLC utilizing the second imaging setup.

IV. Discussion

A. Conclusions

In this work, terahertz (THz) tissue phantoms were successfully developed using solidified emulsions. Three different phantoms were made which mimicked the refractive index and absorption coefficient of fibrous breast tissue, fatty breast tissue and invasive ductal carcinoma (IDC). Additionally, different carbon-based particles were tested for their viability as potential THz contrast agents and a promising candidate was found in onion-like carbon (OLC).

The IDC and fibrous tissue phantoms composed of an emulsion of olive oil and water that was solidified using the solidification agent TX151. The refractive index and absorption coefficient for both phantoms was tuned to match the properties of their respective tissues by altering the amount of olive oil used relative to the amount of water. The initial amount of olive oil to use was predicted using the known properties of the components and Bottcher's equation.

It was predicted that a 10-20 vol.% inclusion of olive oil would be required for the IDC phantom, while 25-40 vol.% and 80-90 vol.% inclusion would be needed for the fibrous and fatty tissue phantoms, respectively. For the IDC phantom, after characterizing potential phantom materials using transmission THz time-domain spectroscopy, it was found that matching both the refractive index and absorption coefficient wouldn't be possible by just changing the amount of olive oil used. To achieve the desired properties, new components like salt were tested but to no avail. However, it was found that by using a 1:1 ratio of olive oil and the neutral detergent used as a surfactant and by using 5mL of oil per 50mL of water, a solid emulsion based phantom could be made that mimicked the optical properties of freshly excised IDC tissue.

Despite the difficulties encountered with the development of the IDC phantom, it was found that materials with a 25 vol.% concentration of olive oil had refractive indices and absorption

coefficients that matches fresh fibrous breast tissue. On the other hand, a fatty breast tissue phantom couldn't be made same solidified emulsion approach as the IDC and fibrous tissue phantoms as the amount of oil required was too high and would prevent solidification by the TX151. Instead lard, cheese and butter were tested as they were commercially available emulsions that could have had similar optical properties as fresh fatty breast tissue. After characterizing the three materials, it was found that butter can act as a THz fatty breast tissue phantom.

One major flaw that was observed with the solidified emulsion phantoms was that over a short period of time after being made, their optical properties would begin to steadily decline. This caused the effective lifetimes of the phantoms to be lower than desired. While it was found that optical properties could be mostly preserved by keeping the phantoms inside sealed plastic bags, the phantoms would still have to be taken out to be worked with. Thus, to increase the inherent lifetime of the phantoms, additions of bleach, guar gum and agar were tested by including them in the fibrous phantom composition and measuring the optical properties of those phantoms after being exposed to open air for twenty-four hours.

The bleach was found to preserve to the refractive index and to a lesser extent the absorption coefficient. However, the bleach also interfered with the solidification of the phantoms and caused instabilities which made any phantom with bleach hard to work with. The guar gum was found to have minimal negative side effects while also allowing for the preservation of only the refractive index. The agar was found to be the best option out of the three as it could preserve both the refractive index and absorption coefficient without any side effects,

To find a contrast agent, two types of carbon-based particles were tested: micrometer-scale diamonds and nanometer-scale OLC. The diamonds were varied in both their size and in what

treatment, if any, was applied to them. To determine the effects of different sizes of diamond, four pristine diamond particles of different sizes (100um, 40um, 20um and 1um) were included in polyethylene tablets. After characterizing the tablets, it was found that the larger diamonds caused scattering of the THz signal which increased the measured absorption coefficient and increased the amount of variance between different measurements. There appeared to be a size limit that would cause the scattering as the 20um and 1um particles provided almost no increases to the absorption coefficient. To determine what effects, if any the two treatments types, irradiation and irradiation followed by being annealed, had on the resulting effects of the micrometer diamonds, diamonds with these treatments and a size of 40um were also incorporated into polyethylene tablets. As the resulting optical properties for both treatments didn't vary from the pristine version, it was determined that the treatments had no effects of the THz optical properties.

To test the effects of the OLC, tablets containing either the 100nm or 200nm OLC were made. It was found that tablets that contained a 1 wt.% addition of the 100nm OLC higher optical properties than the tablets with 1 wt.% of 200nm OLC. This suggests that as the size of the OLC decreases, the increase in optical properties provided increases. Additionally, the 100nm OLC had higher optical properties than the tablets with 10 wt.% of the microdiamonds despite using a lower concentration of particles. This difference increased further when a 10 wt.% addition of 100nm OCL was used.

To verify the effectiveness of the OLC as compared to the microdiamonds, additions of 100nm OLC and 100um pristine diamond were incorporated into IDC phantoms. It was found that despite the highly lossy background material, a 10 wt.% addition of 100nm OLC was still able to provide a large increase to both the refractive index and absorption coefficient while 100umm

pristine diamond particles provided little to no increase. As it could provide a strong increase in the optical properties of IDC phantoms as well as alter THz images of IDC phantoms, 100nmm OLC was determine to be a viable THz imaging contrast agent.

B. Future Work

Continuation of this research will primarily be focused on two main issues: (1) the difficulty of obtaining clear THz images of phantoms and (2) the proper utilization of OLC as a contrast agent. From working with both the IDC and fibrous tissue phantoms, it was found that the phantoms inherently have rough surfaces which prevents them from conforming uniformly to whatever surface they are placed on. This results in small pockets of air forming between the phantom and the polystyrene plate and cause inaccuracies in the image. Future work will need to be performed to identify a method which can reduce or eliminate these air gaps before any phantom imaging work can be done. Current proposed solutions that have yet to be tested include altering the composition of the phantoms, wetting the phantoms and heating the both the phantom and polystyrene plate with a slide warmer prior to imaging.

While the 100nm OLC was found to be the best candidate of the tested particles to act as a THz contrast agent, there is a lot of future work that must be done before it could be used in tissue imaging. From the results of the 100 and 200nm OLC it was hypothesized that as the size of the OLC decreases the effectiveness as a contrast agent increases. By characterizing OLC of smaller sizes, not only can this theory be further tested but a better contrast agent may be found. Once the final particle has been chosen, work will be needed to determine the maximum concentration of the OLC that is physiologically safe. In addition, the molecular mechanism should be investigated to have the OLC specifically target and bind to the cancerous tissue. Additionally, as

OLC can either be bound to the outside of the cell or stored within the cell, the location which provides the best contrast will have to be determined [20]-[23].

V. References

[1] "Health, United States, 2015: With Special Feature on Racial and Ethnic Health Disparities." National Center for Health Statistics [Online]. Available: http://www.cdc.gov/nchs/data/hus/hus15.pdf#019.

[2] "Breast Cancer." American Cancer Society [Online]. Available: http://www.cancer.org/acs/groups/cid/documents/webcontent/003090-pdf.pdf Last revised 13 September 2016.

[3] R. G. Pleijhuis, M. Graafland, J. de Vries, J. Bart, J. S. de Jong, and G. M. van Dam. "Obtaining Adequate Surgical Margins in Breast-Conserving Therapy for Patients with Early-Stage Breast Cancer: Current Modalities and Future Directions." Ann. Surg. Oncol., vol. 16, pp. 2717-2730, July 2009.

[4] S. Glück and T. Mamounas. "Improving outcomes in early-stage breast cancer." Oncology (Williston Park), vol. 24, no. 11, suppl. 4, pp. 1-15, Oct. 2010.

[5] R. G. Pleijhuis, M. Graafland, J. de Vries, J. Bart, J. S. de Jong, and G. M. van Dam. "Obtaining Adequate Surgical Margins in Breast-Conserving Therapy for Patients with Early-Stage Breast Cancer: Current Modalities and Future Directions." Ann. Surg. Oncol., vol. 16, pp. 2717-2730, July 2009.

[6] T. Bowman, Y. Wu, A. Walter, J. Gauch, M. El-Shenawee and L. Campbell, "Time of flight THz imaging of 3D ex-vivo breast cancer tumor tissues," in International Conference on Infrared, Millimeter, and Terahertz Waves, 2015.

[7] T. Bowman, M. El-Shenawee and L. Campbell, "Terahertz Imaging of Excised Breast Tumor Tissue on Paraffin Sections," IEEE Transactions on Antennas and Propagation, vol. 63, no. 5, pp. 2088-2097, 2015.

[8] Ashworth, Philip C., Emma Pickwell-Macpherson, Elena Provenzano, Sarah E. Pinder, Anand D. Purushotham, Michael Pepper, and Vincent P. Wallace. "Terahertz Pulsed Spectroscopy of Freshly Excised Human Breast Cancer." Optics Express 17, no. 15 (2009): 12444-54.

[9] http://www.teraview.com

[10] Ortega-Palacios, R., L. Leija, A. Vera, and M. F. J. Cepeda. "Measurement of Breast - Tumor Phantom Dielectric Properties for Microwave Breast Cancer Treatment Evaluation." 2010 7th International Conference on Electrical Engineering Computing Science and Automatic Control, 2010, 216-19. doi:10.1109/ICEEE.2010.5608579.

[11] Ito, Koichi, Katsumi Furuya, Yoshinobu Okano, and Lira Hamada. "Development and characteristics of a biological tissue-equivalent phantom for microwaves." Electronics & Communications in Japan, Part 1: Communications 84, no. 4: 67-77.

[12] M. Lazebnik, E.L. Madsen, G.R. Frank, and S.C. Hagness, “Tissue-mimicking phantom materials for narrowband and ultrawideband microwave applications,” Phys. Med. Biol., vol. 50, pp. 4245-4258, 2005.

[13] G. C. Walker and E. Berry and S. W. Smye and D. S. Brettle, "Materials for phantoms for terahertz pulsed imaging", Physics in Medicine and Biology, vol. 49, 2004, pp N363-N369.

[14] Reid, C., A.P. Gibson, J.C. Hebden, and V.P. Wallace. "An Oil and Water Emulsion Phantom for Biomedical Terahertz Spectroscopy." 2007 4th IEEE/EMBS International Summer School and Symposium on Medical Devices and Biosensors, 2007, 25-4. doi:10.1109/ISSMDBS.2007.4338284.

[15] Lal, K., and Parshad, R., "The Permittivity of Heterogeneous Mixtures,” Journal of Physics D: Applied Physics 6(11), 1363-1368 (1973).

[16] A. Walter, T. Bowman and M. El-Shenawee, "Development of breast cancer tissue phantoms for terahertz imaging," in Design and Quality for Biomedical Technologies IX, 2016.

[17] Duck, F., [Physical Properties of Tissue], Academic Press, London (1990).

[18] Bockisch, Michael, [Fats and Oils Handbook], AOCS Press, 722-723 (1998).

[19] http://www.adamasnano.com

[20] M. Frasconi, R. Marotta, L. Markey, K. Flavin, V. Spampinato, G. Ceccone, L. Echegoyen, E. M. Scanlan, and S. Giordani, “Multi-Functionalized Carbon Nano-onions as Imaging Probes for Cancer Cells,” Chemistry - A European Journal Chem. Eur. J., vol. 21, no. 52, pp. 19071–19080, 2015.

[21] S. Giordani, J. Bartelmess, M. Frasconi, I. Biondi, S. Cheung, M. Grossi, D. Wu, L. Echegoyen, and D. F. O'shea, “NIR Fluorescence Labelled Carbon Nano-Onions: Synthesis, Analysis and Cellular Imaging,” *J. Mater. Chem. B*, vol. 2, no. 42, pp. 7459–7463, Aug. 2014.

[22] M. Yang, K. Flavin, I. Kopf, G. Radics, C. H. A. Hearnden, G. J. Mcmanus, B. Moran, A. Villalta-Cerdas, L. A. Echegoyen, S. Giordani, and E. C. Lavelle, “Functionalization of Carbon Nanoparticles Modulates Inflammatory Cell Recruitment and NLRP3 Inflammasome Activation,” *Small*, vol. 9, no. 24, pp. 4194–4206, Oct. 2013.

[23] L. Ding, J. Stilwell, T. Zhang, O. Elboudwarej, H. Jiang, J. P. Selegue, P. A. Cooke, J. W. Gray, and F. F. Chen, “Molecular Characterization of the Cytotoxic Mechanism of Multiwall Carbon Nanotubes and Nano-Onions on Human Skin Fibroblast,” *Nano Letters Nano Lett.*, vol. 5, no. 12, pp. 2448–2464, 2005.